CHALMERS
UNIVERSITY OF TECHNOLOGY

Empirical Prediction of Ground-Borne Vibration from Railway Systems

Master's thesis in Sound and Vibration

GUSTAV VÅGFELT

DEPARTMENT OF ARCHITECTURE AND CIVIL ENGINEERING

CHALMERS UNIVERSITY OF TECHNOLOGY
Gothenburg, Sweden 2021
www.chalmers.se

Master's thesis 2021

Empirical Prediction of Ground-Borne Vibration from Railway Systems

GUSTAV VÅGFELT

Department of Architecture and Civil Engineering
Division of Applied Acoustics
Chalmers University of Technology
Gothenburg, Sweden 2021

Empirical Prediction of Ground-Borne Vibration from Railway Systems
Gustav Vågfelt

Supervisors: Mats Hammarqvist & Penka Dinkova, Efterklang - part of AFRY
Examiner: Patrik Höstmad, Department of Architecture and Civil Engineering, Chalmers University of Technology

Master's Thesis ACEX30 2021
Department of Architecture and Civil Engineering
Division of Applied Acoustics
Chalmers University of Technology
SE-412 96 Gothenburg
Telephone +46 31 772 1000

Cover: Eurostar Class 374 high-speed train-set with units 4007 & 4008, near Sellindge in the UK, picture acquired from [1]

Typeset in LaTeX
Gothenburg, Sweden 2021

Empirical Prediction of Ground-Borne Vibration from Railway Systems
GUSTAV VÅGFELT
Division of Applied Acoustics
Department of Architecture and Civil Engineering
Chalmers University of Technology

Abstract

In today's society with the trends of urbanization and rapid growth comes an increasing demand for fast and eco-friendly land travel, with low noise and vibration emission. To predict ground-borne noise and vibration from railway systems, several empirical and numerical models have been developed. Generally, soft ground materials can generate low frequency disturbances in the vicinity of the railway. Stiffer materials can transmit a higher frequency ground-borne noise. Investigations in Sweden have shown that areas with non-stiff soil materials, for example very loose clay, can produce high vibration levels at low frequencies. This is true for some of the soil materials deposited during the melting of the last land covering ice cap, which can be found at various sites throughout Sweden (glacial soils).

This thesis presents an investigation of ground-borne vibration prediction using an empirical model named High-Speed 2 (HS2), developed in two major high-speed railway projects in the United Kingdom. The relevant underlying theory and the prediction model was studied during the initial literature review. The model was programmed in Matlab, and has been utilized to compute predictions of vibration levels arising at a receiver position, as a result of a train passage. A measurement data set of train passages at a Swedish site where the ground material is constituted by glacial clay, has been acquired and processed. This was done in order to compare measurements and predictions for an evaluation of the model's accuracy under Swedish conditions. The findings indicate that the HS2 model can compute relatively accurate vibration level spectra using the default reference data within the model, for the studied case. The average single value difference (vertical particle velocity at the soil surface) between vibration level of predictions and measurements is approximately 2.0 dB, with slight over-estimation of levels for most of the studied frequency range, 6.3 to 250 Hz. This is considered as good accuracy for general noise and vibration assessment. However, it should be noted that these results are based on a comparison of the model with measurement data from one single Swedish site. Further, the model seem to produce lower levels than measurement data at very low frequencies. It is possible that new reference source spectra and propagation terms for soft ground materials would increase the accuracy of predictions for low frequency vibration under Swedish conditions. This would require further measurements for sufficient statistical confidence.

Keywords: Ground-Borne Noise and Vibration, Railway Systems, Soft Ground Materials, High-Speed 2 (HS2) Prediction Model, Low Frequency Vibration.

Acknowledgements

First of all, I would like to thank the supervisors of this thesis project, Penka Dinkova and Mats Hammarqvist, at Efterklang. You have provided valuable insights and guidance during the project. I also want to thank the examiner at Applied Acoustics, Patrik Höstmad, for help and support. Further, I want to thank Jessica Fromell at Efterklang, for enabling this thesis to be conducted in the first place, as well as for her support. A special thanks goes to my father, Kjell Vågfelt, who has given me guidance throughout the project.

Gustav Vågfelt, Gothenburg, June, 2021

Contents

List of Figures

List of Tables

1 Introduction

This chapter is an introduction to the problem investigated within this thesis project. A general introduction of the thesis is presented, along with a specification of the aim and objectives. Demarcations are also covered, as well as a brief examination of societal, ethical and environmental aspects of the work as a whole.

1.1 General Introduction

With the contemporary trends of urbanisation and rapid growth, comes an increasing demand for fast and eco-friendly land travel such as high-speed trains. Railway systems are a source of noise and vibration, and sufficiently low levels in the vicinity of these are a necessity. In urban areas, traffic tend to increase and new buildings occasionally have to be built close to noise and vibration sources. Furthermore, train speeds are generally increasing, which further intensifies noise and vibration issues stemming from railway systems.

Noise and vibration from railways occur partly due to the dynamic interaction between the train and track system, and partly due to aerodynamically induced noise. Noisy on-board equipment can also add to the radiated noise from the train. The excitation of the rails and supporting structure produce mechanical waves that propagate through the ground layers below the track and can in turn excite buildings, producing noise and vibration that can be problematic. The same applies to railway lines in tunnels. In general, railways on softer ground such as sand or clay can lead to low-frequency vibration disturbances in the buildings close by, which is of relevance in frequency range of 1 to 80 Hz [2]. Railways on stiff ground layers give rise to a relatively high-frequent ground-borne noise, with the relevant frequency range being approximately 16 to 250 Hz [2]. Relevant frequencies for ground-borne noise in stiff rock materials can be even higher, up to approximately 1000 Hz. Depending on the building type and design, noise and vibration levels can be attenuated, or even amplified in the structural elements of the building. Older buildings with wooden floors are often susceptible to low-frequency vibration, but also modern lightweight floors with long spans can result in a high response. Furthermore, air-borne sound can also be radiated from the train and the track system which can cause disturbances of e.g. nearby residential areas.

To predict vibration levels from a source to receiver with transmission through a ground layer profile can be rather challenging. This is because of the complex nature of such a dynamic geotechnical problem, with many parameters that influence the calculated results, as well as several uncertainty factors to take into consideration. Nevertheless, there are methods developed to deal with such problems. A ground vibration prediction model is utilized to enable an approximation of vibration levels around the source. Models are often derived empirically from in-situ measurements, but there are also numerical simulation models based on for example the Finite Element Method (FEM), or the Finite Difference Method (FDM). The surface ground vibration level at the receiver position can in combination with building response functions and weighting filters be used to generate predictions of the resulting noise and vibration inside of the building. Either momentarily during a train passage or over a longer time period, due to a certain train flow. However, the models depend heavily on the input parameters defined for the source, propagation path and receiver. Part of the relevant information and input data for a particular case can often be missing, and therefore adequate assumption have to be conducted in order to enable prediction of ground-borne noise and vibration.

In the United Kingdom, in an effort to increase railway capacity, enable higher train speeds and to lower the carbon footprint of domestic and international travel, the High-Speed 1 (HS1) railway project [3] has been implemented. The railway line built within HS1 is a high-speed line from London, England to France through the English channel tunnel, and was finished in 2007. Currently, the first phase of the High-Speed 2 (HS2) project [4] is under way. When finished, high-speed railway lines will connect several major cities in the UK. Both projects have thus far generated research and knowledge within the field of railway induced ground-borne noise and vibration. There is an empirical prediction model developed in the HS2 project, which is published in the documents [5] and [6]. This model is in turn based on a validated model developed in the HS1 project [7] (see also [8]). The HS1 model is based on over 3000 measurements of trains running at speeds of up to 300 km/h, with data from operation on both ground surface level and in bored train tunnels. The model has been validated with in-situ measurements done at two locations in Europe; Muelberg, Germany and Vendome, France [7]. Further, the model has been utilized in various railway and infrastructure projects globally. The aim of the HS2 model is to enable extrapolation of predicted noise and vibration level values to be applicable for train speeds up to 360 km/h. The model has been proven to compute relatively accurate predictions. However, when predicted levels where compared with measurement data from Germany and France in [7], it was shown that the accuracy of the predictions depend on the geological conditions at the site.

This thesis project is conducted in Gothenburg, western Sweden. The HS2 model will be investigated, in particular its applicability and accuracy on Swedish conditions. Soil materials with low stiffness are rather common in western Sweden, and these are generally more susceptible to low-frequency vibration when compared to stiffer soils. Resonances occurring in the soft layer(s) between surface and bedrock can create problematic amplification of these vibrations, which can travel relatively far from the source, particularly at the surface layer, in the form of Rayleigh waves. The problem studied in the thesis is of interest for the future planning, building and operation of new high-speed railway lines. Also, the model can be used when analysing the impact of increased train speeds on an existing track.

1.2 Aim and Objectives

The aim of the thesis is to program the HS2 model in Matlab, and to investigate the applicability and accuracy of the model under Swedish conditions. For clarity, the aim can be rephrased into four questions to be answered based on the thesis investigation;

- **Based on the official High-Speed 2 documents, can the prediction model be implemented in a useful way in Matlab?**
- **Is the High-Speed 2 prediction model suitable for prediction of vibration levels under Swedish conditions?**
- **How accurate are the predictions when compared to measurements, especially regarding soft ground materials and low frequent vibration?**
- **Can the precision of the estimations be increased?**

The model will be analysed and discussed based on comparisons with spectra derived from measurement data. This is done in order to gain a deeper, holistic understanding of the ground vibration phenomenon and vibration prediction, as well as of the model and its parameters, assumptions and potential error sources. The thesis investigation will be implemented by means of a study divided in a number of steps, documented in this report, together with related Matlab scripts. For an explicit overview of the thesis objectives, the following list has been derived.

Objectives:

1. *Execute a thorough literature study within the field of ground-borne noise and vibration, with emphasis on railway induced noise and vibration.*
2. *Study the HS1 and HS2 ground-vibration prediction models and implement the HS2 model in Matlab.*
3. *Compute predictions of train vibration spectra using the HS2 model.*
4. *Acquire train passage measurement data and conduct processing of the data to generate measurement vibration spectra.*
5. *Examine the accuracy HS2 predictions by comparing the estimated vibration spectra with measured spectra.*

6. *Investigate assumptions, uncertainties and potential error sources within the model, as well as for measurement procedures and data processing. Possibly discuss and propose adaptation of the model in order to increase the accuracy of predictions.*

1.3 Demarcations

This section declares the demarcations set for the thesis project. There are several fields of science and engineering involved in the chosen topic. Therefore, demarcations are needed due to the limited time-frame. The following list presents the demarcations.

1. *The study of ground-borne vibration and the HS2 model will solely deal with the case of surface running trains and mainly low-frequent physically perceptible vibration.*

2. *The HS2 model calculation steps for applying building response functions and weighting filters, as well as for conducting averaging over longer time-spans (due to expected train flows) will only be described in the report, not implemented in the Matlab script. Only prediction of vibration level spectra up until a receiver position at ground surface is conducted in the thesis.*

3. *Direct air-borne noise from railway systems is excluded in the analysis, it is only mentioned briefly within the Theory section.*

4. *A comprehensive geological study with seismic measurements is considered out of scope for this thesis, due to the limited time-frame. Only basics within geology and soil properties will be explained in a nutshell. Basic information on geological conditions at measurement sites are acquired through the Geological Survey of Sweden (`www.sgu.se`).*

1.4 Societal, Ethical and Ecological Aspects

With this thesis project, as with everything produced on a public and/or professional level, comes responsibilities in ensuring that the project meet the rules and norms of societal, ethical and ecological values.

With this specific project, the societal aspect one could argue is rather obvious. The ultimate aim of the work is to enable a higher quality of living for people residing close to railway systems. It is also to enable investigation of suitable locations of for example laboratories that operate vibration sensitive equipment. This is important in a society with increasing urbanisation. However, erroneous results of the calculations could in worst case create issues for stakeholders involved in planning, building and operation of railway systems, as well as for residents of buildings in the vicinity of railway lines. Further, animals and livestock can be affected by the vibration from railways.

Ethical concerns are a bit more diffuse to pin point, however, it is of upmost importance that the published results and conclusions will provide a basis for taking responsible and reasonable decisions when e.g. planning a new railway track, or when increasing train speeds on existing tracks. Ethics is a complex topic with many factors involved, and can be rather subjective. Nevertheless, it is of importance to keep this in mind when ultimately publishing the work.

As for the ecological aspect of the thesis, the findings of the thesis could be utilized to plan a growing network of high-speed train tracks, enabling fast and a more environmentally friendly travel than compared to e.g. air travel. Whether construction of an expanded railway net would be positive or negative in a ecological aspect for the society as a whole, is a topic of discussion. Further, predictions of noise and vibration enable planning of noise and vibration mitigating measures, which can be positive for the nearby environment of major transportation systems.

2

Theory of Ground-Borne Noise and Vibration

This section presents fundamental theory behind the phenomenon of ground-borne noise and vibration induced by railway systems. It deals with basics of acoustic wave propagation in solid materials and covers some aspects of geology and soil properties relevant for the investigation. Vibration generating mechanisms of railways are explained, along with general descriptions of relevant track-train dimensions and railway track system types. Furthermore, some words on ground vibration measurements, weighting filters and receiver properties such as building and human response, are presented. This section is meant to function as background information for a general understanding of the complex phenomenon of ground-borne noise and vibration, some of the theory is not directly used within the analysis section of the thesis.

Ground-borne noise and vibration can arise from various types of sources, from man-made sources and from naturally occurring vibration phenomena like earthquakes. The excited waves will propagate through the ground's soil and rock layers, ultimately reaching the receiver in the form of either low-frequent vibration or ground-borne noise, or as a combination of the two. Ground-borne noise and vibration occupy different frequency ranges, with some overlapping of their respective range. According to the international standard "Mechanical vibration – Ground-borne noise and vibration arising from rail systems", ISO 14837 [2], ground-borne vibration and ground-borne noise are divided into the ranges of 1 to 80 Hz, and 16 to 250 Hz respectively. Generally, propagation through stiffer soil materials give rise to ground-borne noise. For stiff rock materials, ground-borne noise can propagate with frequencies higher than 250 Hz. According to ISO 14837 [2], the relevant frequency range for effects on buildings is between 1 to 500 Hz. For less stiff ground material types such as clay or sand, problems can arise with respect to low-frequent vibration.

There are several wave types that occur within solid materials, of which the compression wave, shear wave and Rayleigh wave are of importance when dealing with ground-borne noise and vibration. These are elastic waves that are often referred to as ground-borne waves or seismic waves (forms of mechanical waves). Other types of waves that can arise are e.g. Love waves and Stoneley waves [2]. The relevant wave types of ground-borne vibration are explained further in Section 2.1. The following sections are based on information provided in [2], [9] and [14], among other resources.

2.1 Elastic Waves in Solid Materials

An acoustic wave propagates through a solid medium as a oscillating, periodic motion of the material particles. The particles can exhibit several types of motion relative to one another, i.e. different wave types are needed to describe different oscillating motions in a solid material. Due to inter-molecular forces between the molecules in a solid medium, an oscillating motion will elastically move particles back and forth, through compression, rarefaction and/or shearing. A gas or liquid will not display shear tension, hence, no shear waves can propagate through such a medium. Within soil mechanics and wave propagation, the stress-strain relation dictates how the material can be modelled. Seismic activities like collision of tectonic plates can produce propagating waves of such magnitude that plasticity and non-linearity have to be considered. However, analysis of wave propagation in ground materials is simplified with the assumption of a linearly elastic material, which most often is the case for small strain values produced by man-made sources, such as roads or railways. Further, a homogeneous material is generally easier to model, which is not always the case for natural ground layer materials. However, this depends on the considered wavelength in relation to the ground material grain size. For a very low frequency with a long wavelength, some materials can be assumed homogeneous at this frequency. However, homogeneity might be an unsuitable assumption for a complete ground layer profile, which can consist of several different materials deposited on top of one another.

The following sections present the relevant seismic wave types and propagation phenomena needed to describe ground-borne noise and vibration induced by railway systems.

2.1.1 Seismic Wave Types

As mentioned previously, there are many types of elastic waves that can be excited and propagate through a solid material. Energy produced by the vibration source is transferred to the surroundings through these wave motions. They can be divided into two main categories, body waves and surface waves. Normally, a combination of both these wave types arise when a ground material is excited, and the different waves propagate at different speeds depending on material properties. Loose ground materials tend to produce lower wave propagation speeds, and stiffer ones produce higher. Furthermore, surface waves tend to occur in close proximity to a boundary surface, e.g. in the top ground layer at the intersection between the ground material and surrounding air.

The category of body waves can be further divided into two separate type of waves, namely compression and shear waves. These waves propagate further down into the ground's different layers, compared to surface waves. When energy is transferred through a solid medium by the compression wave (also referred to as primary wave, pressure wave and P-wave), the material particles move in an oscillating motion of compression and rarefaction. The particles are displaced in the same direction as the propagation direction of the wave, forming a longitudinal motion as illustrated in Figure 2.1 below.

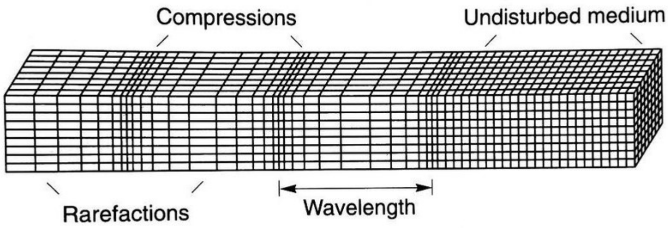

Figure 2.1: Illustration of the dynamic movements of a compression wave [10]. Figure adopted from [11].

The compression wave has a higher propagation speed compared to the shear wave (shear wave explained further in following paragraphs). Usually, these waves arrive first when observing ground vibration at some arbitrary distance away from the source. The speed of the compression wave depend on the medium properties in which it is propagating. Equation 2.1 can be used to determine C_p, i.e. the speed of the compression wave in m/s,

$$C_p = \sqrt{\frac{\lambda + 2\mu}{\rho}}, \tag{2.1}$$

where λ and μ are the so-called Lamé constants and ρ is the material density in kg/m^3. The Lamé constants can be determined by utilizing the following two equations,

$$\lambda = \frac{\nu E}{(1+\nu)(1-2\nu)}, \qquad \mu = \frac{E}{2(1+\nu)}, \tag{2.2}$$

where ν is the Poisson's ratio and E is the Young's modulus, measured in Pa. μ is also denoted as the shear modulus G. Therefore, the equation for the Lamé constant μ can be used to calculate a material's shear modulus if the Young's modulus and Poisson's ratio are known.

By inserting the Lamé constants into Equation 2.1, the following expression for the propagation speed of the compression wave can be defined,

$$C_p = \sqrt{\frac{E(1-\nu)}{\rho(1-2\nu)(1+\nu)}}. \tag{2.3}$$

The shear wave (also referred to as secondary wave and S-wave) is a so-called transverse wave, in which the particle motion of the medium is perpendicular to the propagation direction of the wave. This movement is illustrated in Figure 2.2. Furthermore, the movement of a shear wave can be divided into two components, one in the horizontal plane (SH), and one in the vertical plane (SV).

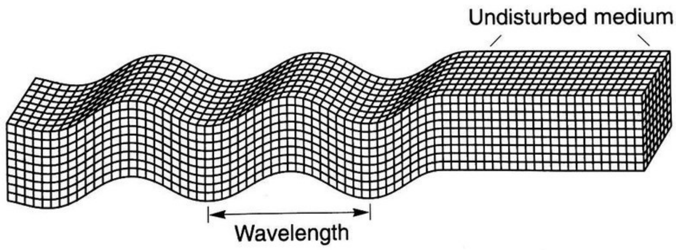

Figure 2.2: Illustration of the dynamic movements of a shear wave [10]. Figure adopted from [11].

The propagation speed of the shear wave, denoted C_s, is determined by the following equation,

$$C_s = \sqrt{\frac{\mu}{\rho}}. \tag{2.4}$$

By utilizing the expression for the Lamé constant μ, the following expression for C_s can be stated,

$$C_s = \sqrt{\frac{E}{\rho 2(1+\nu)}}. \tag{2.5}$$

The second main category of waves in solids are surface waves, which propagate (depending on e.g. the ground layer profile and the wavelength considered) in the top most ground layer, bounded by the surrounding air. These waves can also occur at the interface between two solid materials with drastically different properties. The amplitude of the surface waves decrease significantly with depth from the interface between the media. However, these waves are typically the most critical when analysing a ground-borne noise and vibration problem in a building. This is because surface waves tend to propagate further than body waves, due to the fact that the geometrical attenuation for body waves is generally larger (attenuation and damping is further discussed in Section 2.1.6). This means that for a general case, surface waves carry energy farther away from the source.

The Rayleigh wave is a seismic wave type discovered by Lord Rayleigh in 1885. It is a surface wave where the particle motion oscillates in an elliptical pattern, see Figure 2.3. The motion incorporates both a transverse and a longitudinal component. According to the ISO standard 14837 [2], the Rayleigh wave is usually the most critical wave type with regards to vibration stemming from surface running trains, or from trains on elevated structures such as a track system on a railway embankment.

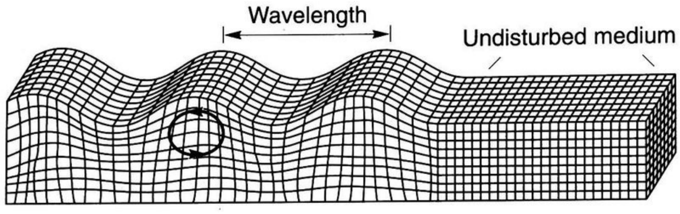

Figure 2.3: Illustration of the dynamic movements of a Rayleigh wave [10]. Figure adopted from [11].

The propagation speed of the Rayleigh wave is usually slightly lower, but close to that of the shear wave. For materials with ν in the range of 0 to 0.5 (see Table 2.3), the Rayleigh wave speed, denoted C_R, can be approximated using the following expression:

$$C_R \approx \frac{0.87 + 1.12\nu}{1 + \nu} C_s, \tag{2.6}$$

as described by Bergmann and Hatfeild in 1938 [13].

There are further types of seismic waves occurring within solid materials. However, the following two wave types are only described briefly as they only propagate under certain conditions, and are not of significance for the studied case of this thesis.

The Love wave, which also bears its discoverer's name (Augustus Edward Hough Love, who predicted the waves existence mathematically in 1911), is a surface wave that produce a particle motion that can be described as a horizontal shift at the boundary between the two media, a shearing motion of the top surface layer. In layman terms, the motion is rather similar to that of a mowing snake, an S-shaped oscillating movement in the horizontal plane, see Figure 2.4.

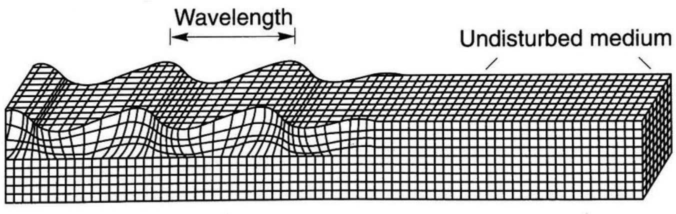

Figure 2.4: Illustration of the dynamic movements of a Love wave [10]. Figure adopted from [11].

Furthermore, so-called Stoneley waves can occur at boundaries between two different media, therefore referred to as boundary waves or interface waves. These waves propagate along the boundary plane between the two media, and are guided along the interface. The particle motion is similar to that of the shear wave, with propagation direction along the boundary plane and particle motion perpendicular to this plane.

2.1.2 Ground Layer Resonance

When studying a case of for example two loose ground materials on top of stiff bedrock, it can with some simplifications be modelled as a two degree of freedom mass spring system. This means that there will be inherent resonances and anti-resonances depending on the excitation of the ground layers, as well as the properties of the materials, and the geometry. This is illustrated in Figure 2.5.

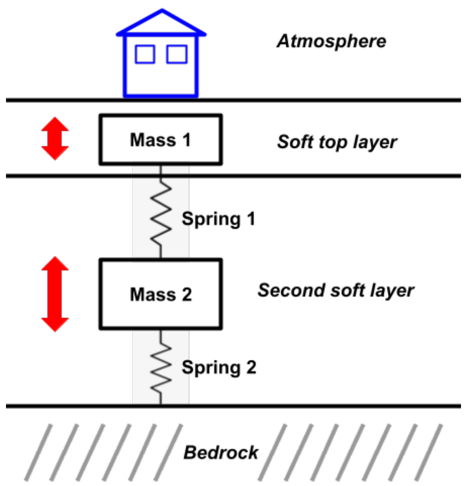

Figure 2.5: Illustrative figure of a two degree of freedom mass spring system.

If a frequency component of the vibration spectrum generated by a railway line coincide with an eigenfrequency of the particular ground layer formation, or a floor span inside a building, large vibration amplitudes can arise. If this is the case, a resonance occur, where a relatively weak excitation force can produce a high response. The eigenfrequencies for a single homogeneous soil on top of stiff bedrock can be determined using the following expression,

$$f_n = \frac{(2n+1)C_s}{4h}, \tag{2.7}$$

where f_n is the n^{th} eigenfrequency in Hz, C_s is the shear wave speed in m/s and h is the depth of the soil layer in metres [14]. This equation holds for amplification that occur due to SH-waves propagating vertically. Usually, the eigenfreqeuncy of lowest order (n=0) is the most critical. With increasing order of eigenfrequency, the amplification of the wave generally decreases. The wavelength of the particular frequency can be derived using the following equation,

$$\lambda = \frac{C}{f}, \tag{2.8}$$

where λ is the wavelength in metres, C is the propagation speed of the wave in m/s and f is the frequency in Hz.

Due to the fact that the ground layer profile can be very different depending on location, the presented mass spring analogy might not be sufficient to describe the dynamic movements of a more complex system. The analogy does not hold if there are many inconsistencies, multiple heterogeneous layers and drastic changes in topography, etcetera. Another example that complicates analysis is if the distance to bedrock decreases gradually. Then, resonances and anti-resonances can be shifted upward in frequency, potentially resulting in a higher response at these shallower depths of the overlying layers. This also means that if an energy is able to be transferred over long distances, vibration disturbances can arise at a distance relatively far away from the source. This can be the case of Rayleigh waves excited by a line source (further information on surface wave propagation effects in Section 2.1.6).

2.1.3 Reflection, Refraction and Wave Coupling

When acoustic waves propagate between two media, the phenomena of wave reflection and refraction arise. Interaction between reflected and refracted waves and so-called wave coupling at boundaries can generate wave types not present before, as well as leading to a complicated interference pattern within the ground layer profile. Moreover, the interference can act both constructively and destructively, increasing or decreasing the amplitude of the propagating waves.

The mechanism of acoustic reflection arise from a change in impedance between two media. The reflection of the wave occur at the boundary between two different media, and the angle is determined by the incident angle of the wave. However, in a real case there might not be a definitive boundary between two soil types of different density, but rather a gradual shift in density. Also, the ground layer formation could exhibit a convoluted geometry, resulting in difficulties of explicitly modelling such a reflection phenomenon. The second mechanism, called refraction, is a change in propagation direction when the wave enters a medium with different properties. Similar to the refraction of light when propagating from air to water, the acoustic wave propagate in a slightly different direction rather then being reflected. An illustration of reflection and refraction is presented in Figure 2.6.

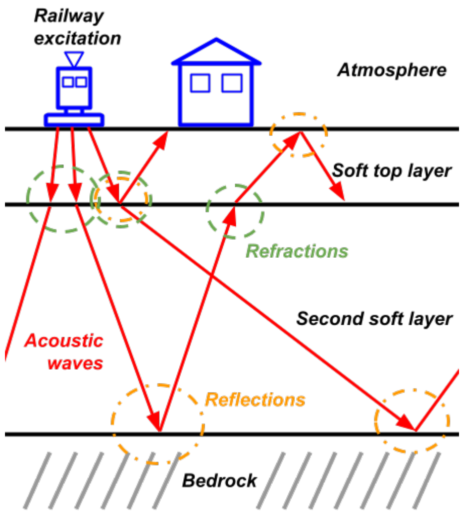

Figure 2.6: Illustrative figure of seismic reflection and refraction.

At the interface between two ground layers, coupling between different wave types can occur when a wave is propagating through the boundary. For example, P- and S-waves are coupled at the interface. An incoming P-wave could be transmitted into a refracted SV-wave and P-wave, as well as reflected as an SV-wave and a P-wave. Therefore, as mentioned previously, wave types not present before can arise from the mechanism of wave coupling at boundaries. An illustrative example of wave coupling at an interface between two media is presented in Figure 2.7.

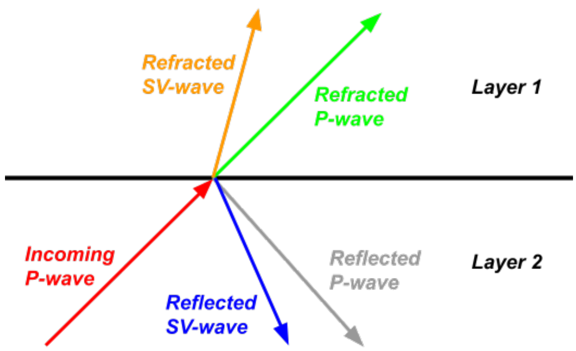

Figure 2.7: An example of wave coupling at an interface between two media. Figure adopted from [14].

The phenomena presented Figure 2.7 occur at all layer interfaces, and for both P- and S-waves. If there are multiple ground layers at the site under consideration, which often is the case in real life, the result is a complicated wave pattern consisting of several different wave types with varying amplitude and phase.

2.1.4 Diffraction and Scattering

There are several mechanisms that add to the complicated nature of wave propagation in solids. Diffraction and scattering are two more relevant mechanisms that affect the wave field produced in soil and rock materials that are excited by dynamic forces. In a natural environment the ground materials are often compounds of multiple, typically heterogeneous layers, and inconsistencies like rocks and other formations within the layers are not uncommon. These are typically zones where these mechanisms can arise.

Diffraction can arise at the presence of for example an object, or at a drastic change in the topography. In a nutshell, diffraction is the bending of acoustic waves around an anomaly. Diffraction therefore causes a spatial redistribution of the acoustic energy. Further, the wavelength of the propagating waves in relation to the size of the object will also have an impact on the redistribution of the wave field.

Scattering also refers to a form of spatial redistribution of acoustic energy in the propagation medium. Scattering can arise when a seismic wave front is confronted with an obstacle or drastic changes in the soil properties. It can be described as splitting of the wave front into fragments of the original wave front, with varying phase and propagating in several directions away from the object/anomaly. Wave coupling can also occur when a seismic wave is scattered, i.e. that a scattered wave can consist of different seismic wave types.

2.1.5 Dispersion

Dispersion refers to frequency dependant wave speed, i.e. different frequencies (or wavelengths) of a wave front of the same wave type propagate at different speeds. As declared in Section 2.1.1, the wave speed depend on the material properties, and for a homogeneous soil, seismic waves travel at the same speed. However, it is common for ground layer profiles to exhibit increasing stiffness with depth, which can lead to dispersion of Rayleigh waves. Dispersion of surface waves will result in longer wavelengths propagating at a higher speeds than shorter wavelengths. To describe the propagation of the "wave package" produced due to dispersion, two categories of propagation speeds are used describe the phenomenon, namely group speed and phase speed. The group speed, here denoted as C_{Gr}, is the propagation speed of the overall envelope of the wave package, and the phase speed, denoted C_{Ph}, is the propagation speed of a particular phase. Both quantities can be determined from the difference in distance and phase between two measurement positions using the following equations,

$$C_{Gr}(f) = \Delta r \frac{2\pi f}{\Delta\phi}, \qquad\qquad C_{Ph}(f) = \Delta r \frac{2\pi\partial f}{\partial\Delta\phi}, \tag{2.9}$$

where f is the frequency, Δr is the difference in distance and $\Delta\phi$ is the phase difference between the measurement positions [14].

2.1.6 Geometrical Attenuation and Material Damping

When acoustic waves propagates through a medium, energy is dissipated and the intensity of the wave motion decay with distance. The amount of dissipated energy is dictated by both the material's inherent properties (the damping coefficient, here referred to as α), as well as the geometry of the propagation medium. One can therefore differentiate attenuating effects into material damping and attenuation by means of geometrical spreading of the acoustic waves. The following paragraphs describe both mechanisms and are based on information provided in the document [14].

Geometrical attenuation is due to spreading of the propagating waves over an increasingly larger volume away from the vibration source. The attenuation depend on the type of source as well as the geometry itself. The following expression for geometrical attenuation in a half space of perfectly elastic material for surface and body waves was derived by Horace Lamb in 1904 [15],

$$\hat{v} = \hat{v_1} \left(\frac{r_1}{r}\right)^m, \tag{2.10}$$

where $\hat{v}$ is the top vibration amplitude at distance r metres from the source, $\hat{v_1}$ is the top vibration amplitude at distance r_1 from the source and m is a constant depending on the wave type, source type and propagation path of the wave, see Table 2.1. The fifth column in Table 2.1 presents the factor of which the propagating wave is decaying by. These factors are derived using the respective m values and Equation 2.10.

Table 2.1: Values of the constant m used in Lamb's equation for geometrical attenuation. Table adapted from [14].

Wave propagation	Source type	Wave type	m	Factor of decay
Along surface	Point source	Body wave	2	$1/r^2$
Along surface	Point source	Surface wave	0.5	$1/\sqrt{r}$
Inside of half space	Point source	Body wave	1	$1/r$
Along surface	Line source	Body wave	1	$1/r$
Along surface	Line source	Surface wave	0	No decay
Inside of half space	Line source	Body wave	0.5	$1/\sqrt{r}$

Material damping can be described as a mechanism which transforms kinetic energy into heat by means of friction between the particles of the material. It is determined by the material parameter α, which may be frequency dependent. Further, damping in soil materials can exhibit viscous behaviour, depending on e.g. water saturation. Viscous damping refers to damping that is proportional to the velocity of the system. According to [14], the material damping decrease partially with increasing frequency and partially with increasing propagation speed of the waves (meaning that the damping is greater for loose soils compared to stiffer ones). Dissipated energy due to material damping can be interpreted as energy loss per wave cycle. This means that the intensity of lower frequencies with longer wavelengths do not decay as fast has for higher frequencies.

To determine the total attenuation of the propagating waves including both geometrical decay and material damping, the following version of Lamb's equation can be utilized,

$$\hat{v} = \hat{v_1} \left(\frac{r_1}{r}\right)^m e^{[-\alpha(r-r_1)]}. \tag{2.11}$$

Typical values for the damping coefficient of different ground materials at 50 Hz is presented in Table 2.2.

Table 2.2: Typical values of the damping coefficient α at 50 Hz for different material types. Table adapted from [14].

Type of material	Damping coefficient α
Soft soils*	0.1 - 0.3
Firm soils**	0.03 - 0.1
Stiff soils***	0.003 - 0.03
Bedrock	< 0.003

**soft soils: organic soils like peat, silt and ooze, loose to mid stiff clay and very loose sand (a shovel is easily pressed through).*

***firm soils: solid clay and loose to mid stiff non-cohesive/friction soils (may be excavated with a shovel).*
****stiff soils: very stiff clay and non-cohesive/friction soils, as well as relatively stiff weathered rock materials (too stiff for excavation using a shovel).*

Note: ground materials are further discussed in Section 2.2.

2.2 Fundamentals of Ground Materials and Geotechnics

In order to achieve a holistic understanding a ground vibration problem, geotechnical aspects have to be considered. There are many factors that determine how ground materials behave when a dynamic load is applied. For example, the saturation of water inside of the ground material influences the propagation speed of the ground-borne waves, increasing material stiffness with depth may cause dispersion and other phenomena. The following paragraphs present some of the basics within soil and rock mechanics relevant to this study, in a nutshell. Further, a compilation of properties for several generic ground material types is also presented.

Ground materials can exhibit a wide variety of types, with varying properties. The ground material categories of rocks and soils behave rather differently to excitation, e.g. the stiffness and internal material damping differ. As mentioned in the Introduction, harder rock materials typically produce a higher frequency ground-borne noise when excited. Loose soils like clay transmits low frequency vibration more efficiently, whilst high frequencies are attenuated, when compared to a harder rock material. In a typical case, the ground layer profile incorporates a few metres of soil, drift and weathered rock (weathering can be described as breakdown of ground material due to physical and/or chemical processes), on top off bedrock [16]. Within geotechnics, the ground layer profile is sometimes referred to as the geological macro-structure, which is developed through natural geological processes, like for example deposition of sediments during melting of glacial ice. Typically, the material density increases with depth in a geological macro-structure due to natural consolidation over time. The inherent geometry inside of a material with regards to particles/grains and pores is called the micro-structure of a ground material. Soils are compounds of weathered minerals, organic matter, water, air and more. They may be further divided into topsoil rich in organic matter, and subsoil with more clay-like constituents. Drift refers to relatively young deposited sediments, consisting to large extent of clay, sand and coarse broken rock materials [16].

Soil is the common name for the softer materials of the earth's crust. A soil material typically consist of solid grains with intermediate pores containing water and/or air. It can therefore be considered as a three-phase material [17], see Figure 2.8.

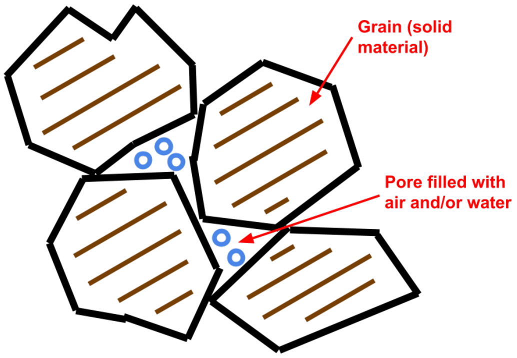

Figure 2.8: A figure illustrating a typical micro-structure of a soil material. Figure adapted from [17].

Soils can be divided into two main categories, namely organic soils and mineral soils. Organic soil is defined as materials with more than 20 % organic material (stemming from e.g. degraded plants and animals), and can be relatively porous [18]. Examples of organic soils are peat and muck. Common mineral soils are sand, gravel and moraine. To further characterise these ground materials, soils can be divided into cohesive and non-cohesive soils. In a non-cohesive soil the friction between the particles is the mechanism that binds the soil particles together. Examples of these material types are sand and gravel. The mechanisms that binds together the particles of a cohesive soil are both friction and inter-molecular forces, attracting the particles to one another. Examples of cohesive soils are silt and clay. Obviously, ground layers can consist of a mixture of several materials types, and their mechanical behaviour under load can vary significantly. Generally, ground materials are stiffer under compression load, when compared to shearing. Further, a dry soil can be relativity stiff whilst a water saturated soil can be rather soft and be prone to deformation. Moreover, the amount of water inside of a ground material can affect the damping of ground-borne waves. ISO 14837 [2] states that water saturation in a porous soil can produce viscous damping at high frequencies.

In Table 2.3, material properties of a selection of generic ground materials are presented. The information in the table is based on Head and Jardine's report from 1992 [19].

Table 2.3: Typical values of ground material properties. Table adapted from [14].

Material:	C_p & C_s:	ν:	ρ:	G_{max}:
Loose sand	1450-1550 & 100-250	0.48-0.50	1.5-1.8	15-110
Medium-firm sand	1500-1750 & 200-350	0.47-0.49	1.7-2.1	70-250
Stiff sand	1700-2000 & 350-700	0.45-0.48	1.9-2.2	230-1000
Loose clay	1450-1550 & 80-180	0.47-0.50	1.6-2.0	10-65
Medium-firm clay	1500-1700 & 180-300	0.47-0.50	1.7-2.1	55-190
Stiff clay	1600-1900 & 300-500	0.47-0.50	1.8-2.3	160-450
Sandstone	1400-4000 & 800-2000	0.25-0.35	2.0-2.4	1300-9500
Limestone	2100-6000 & 1200-3000	0.25-0.35	1.8-2.5	2600-20000
Gneiss	3500-7000 & 2000-3500	0.25-0.35	2.2-2.6	8500-32000

In Table 2.3, C_p and C_s are the propagation speeds in m/s of the compression and shear wave respectively, ν is the Poisson's ratio, ρ is the material density in Mg/m^3 and G_{max} is the shear modulus in MN/m^2. Note: the expression for the Lamé constant μ, presented in Equation 2.2, can be used to derive the Young's modulus of the materials presented in Table 2.3.

Geological maps can be used in order to gain understanding of the geological conditions at the site under consideration. These maps can include information on e.g. generic ground layer material types and layer depths. In Sweden, the Geological Survey of Sweden [20] has developed an online map application that provides information on ground material type, layer depth (estimated depth to bedrock), ground water properties at the site and more [21]. However, geological maps should be used with caution as they are based on discrete sampling positions. Since soil and rock are natural materials stemming from complex geological processes, there will always be some uncertainty when attempting to map geological conditions, or when trying to explicitly quantify the mechanical behaviour of such a material. If there is a need for an in-depth examination, a geological investigation of the prevailing conditions at site may be conducted, which can be both expensive and time consuming. Geological/seismic measurements will not be discussed in this thesis. For the interested reader, information on this topic can be found in the following document, provided by the Swedish Geological Institute: [22].

2.3 Railway Induced Ground Vibration

The phenomenon of ground-borne noise and vibration generated by railway systems is rather convoluted, encompassing a dynamic system with multiple parameters and many factors at play. The dimensions and masses of the train vehicles, the train-set configuration, track-bed construction, train speed and ground material properties at the site under consideration, all affect the resulting vibration. The following sections discuss relevant dimensions of the train and track, vibration inducing mechanisms, ground vibration build up due to the so-called ground vibration boom phenomenon, as well as some general information on railway track types and the supporting substructures. This section is based on information provided in the resources [2], [9], [28], [29] and [30].

2.3.1 Some Words on Train-Track Design Relating to Noise and Vibration

Some excitation mechanisms of railway systems are directly related to the track and train designs. For example, the total weight of the vehicle, it's so-called unsprung mass, and the axle spacing's influence the excitation of the track and track-bed. The relevant train-track dimensions that are related to vibration generating mechanisms are well documented in ISO 14837 [2].

A train configuration usually consist of multiple coupled vehicles with either a diesel or electric locomotive powering the complete set. Sets can vary from a few coupled vehicles to a relatively large number of vehicles, with total lengths of several hundred meters. As an example, the Three Capitals Eurostar 373 high-speed train set has a total length of up 387 metres, and incorporates two powered cars and 18 passenger vehicles of different types, weighing approximately 750 tonnes, see Figure 2.9 below.

Figure 2.9: An 18 passenger car Eurostar train on the LGV Nord high-speed railway line at Moussy-le-Neuf, France. Figure acquired from [23].

A train design with two bogie's per vehicle is rather common. Each bogie usually incorporates two axles with one set of wheels each. The mass of the axles, wheels and all equipment mounted on these, which are undamped and directly in contact with the rail head through the wheel treads, are together referred to as the railway vehicle's unsprung mass. This mass is relevant to one of the vibration generating mechanisms, explained further in Section 2.3.2. The total mass of the vehicle as well as the weight of the bogie installation above the wheel suspension also affect the vibration generation. In Figure 2.10, the relevant train dimensions (and one dimension of the track system) for the so-called parametric excitation mechanism are presented, as stated in ISO 14837 [2].

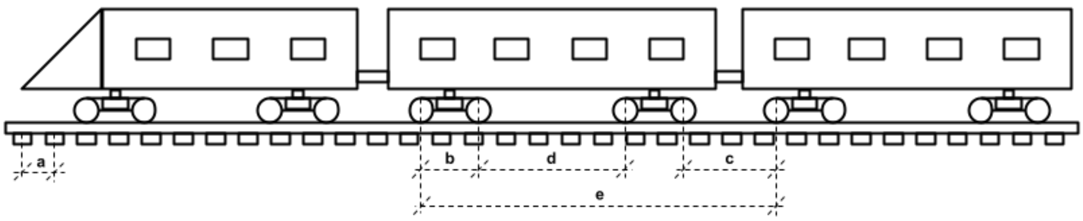

Figure 2.10: Relevant train dimensions for the parametric excitation. Source: [2].

Dimension a of Figure 2.10 is the only one relating to the rail system. The other dimensions relate to the train-set. These dimensions are described in Table 2.4.

Table 2.4: Description of the dimensions of Figure 2.10. Source: [2].

Dimension	Description
a	sleeper spacing of track system
b	distance between intra-bogie axles
c	distance between inter-bogie axles
d	distance between intra-vehicle axles
e	distance between inter-vehicle axles

As previously stated, the configuration of the train set influence the generated vibration spectrum. If a train set consist of multiple vehicles of which the majority is of passenger type that possesses different axles spacings than the locomotive, these spacings will generate the prominent frequency components when studying the parametric excitation spectrum of the complete train passage.

For an overview of an exemplary Swedish train set, a side view of the Regina electric train is presented in Figure 2.11. This train has a type of combined locomotive/passenger car and a intermediate passenger car, for the three car train set configuration. Technical information on the train set is provided by the manufacturer Bombardier [24].

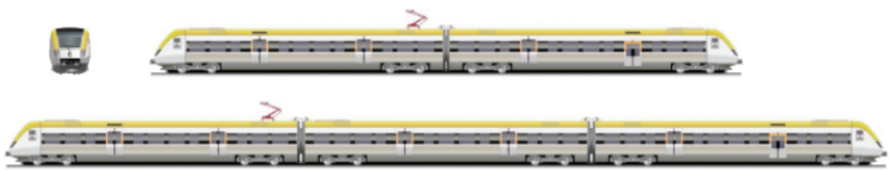

Figure 2.11: Side view of the Regina train under operation in Sweden. Figure acquired from [24].

The bogie wheelbase of the Regina train is 2.7 metres and the centre distance between two bogies on either car type is given to be 19 metres. For new standard ballast track built in Sweden, the criteria for sleeper spacing is 600 millimetres [25] (the standard rail gauge of Swedish railways is 1435 millimetres). This would mean that, according to the dimensions presented in ISO 14837, dimension a would equal 0.60 metres, dimension b 2.7 metres and dimension d would equal 16.3 metres. Dimensions c and e could possibly be approximated by measuring in a side view picture of the train set, with the known bogie wheelbase dimension (millimetres per pixel). The two car and three car versions have total empty weights of 120 and 165 tonnes respectively. The unsprung mass is not specified in the manufacturer's document.

Figure 2.12: A bogie installation on a Chinese CR200J train. Figure acquired from [26].

Figure 2.12 presents a picture of a typical train bogie installation. The car is connected to the bogie via two suspension sets. The suspension at the axle is referred to as the primary suspension, and the one directly connected to the carriage at the middle of the bogie is the secondary suspension. The rails are supported by sleepers on ballast, which are loaded by a part of the mass of the car-body, bogie frame, the unsprung mass and all other equipment included in the bogie installation. These properties of the train (masses and lengths), are relevant to some of the vibration generation mechanisms of the train. How the railway vehicle interacts with the track through the bogie installation has been schematically represented in Figure 2b of ISO 14837 [2], part 1 (see also Figure 2.13). This is a description of the actual noise and vibration source that is constituted by the car body, bogie installation and track system, plus the supporting ground. Vibration inducing mechanisms of trains are further discussed in Section 2.3.2.

2.3.2 Vibration Inducing Mechanisms of Railway Vehicles

There are several vibration generating mechanisms related to railway systems, which are all dependant on the train speed. Generally, a higher train speed produces increased vibration. However, there are examples where slow and heavy freight trains produce high vibration levels. The separate mechanisms all contribute to the generated vibration spectrum, although their respective magnitude can vary. In the following paragraphs, the main ones are described and additional mechanisms are also mentioned. It should be noted that some of the mechanisms are not yet fully understood, as stated in ISO 14837 [2], and further research within this topic is needed.

The so-called quasi-static excitation can be interpreted as the excitation caused by the train's moving load under the wheels. The mass of the railway vehicle applied to the rails causes a displacement in the rails and the supporting infrastructure. When the train is running, this displacement is shifted along the rail, causing an excitation of bending waves in the rails, which are transmitted to the substructure of the track and further to the surrounding ground layers. When imagining the effect of the moving load(s) at a single point in the supporting structure, a time-varying deformation at this point is generated, i.e. dynamic movements of the supporting structure occur. Obviously, the frequency of this excitation is dependant on how fast the train is moving, as seen from the fixed point. This excitation mechanism is usually related to very low frequent vibration. In layman's terms, and rather exaggerated, quasi-static excitation can be thought of as the train wheel's tread causing a deflection in the rail and supporting structure, making it constantly "run uphill" whilst the train is moving, see Figure 2.13.

Figure 2.13 presents a simplified illustration describing some aspects of the train vibration source. It highlights the quasi-static mechanism, but also indicates the workings of further mechanisms. The roughnesses of the wheel and rail are also illustrated in the figure, which depend on manufacturing processes (and design tolerances), as well as wear and maintenance of the rolling stock and track. Corrugation of both wheels and rails can also contribute to the overall roughness profiles. The roughness profiles of the wheel tread and rail head interacts when a train is rolling, and causes variations in contact force, which produce excitation of the track-structure. This mechanism is referred to as roughness excitation. The contribution from roughness depend on many variables, but can be approximated using a so-called effective roughness spectrum as a reference baseline in prediction of ground vibration from railway vehicles. Such a spectrum is typically based on measurements of real rolling stock and rails, and incorporates an effective roughness amplitude that is produced by roughness excitation at a certain wavelength.

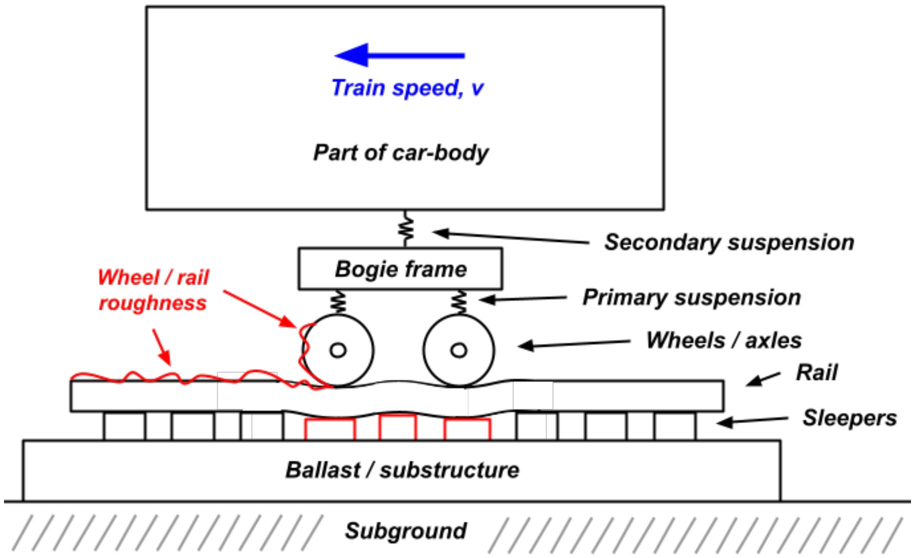

Figure 2.13: A rudimentary, schematic model of the noise and vibration source (excluding noise arising from other on-board equipment and airflow).

Parametric excitation occurs when a train is running at some speed, v m/s, on top of the rails which are supported by sleepers, separated by a distance depending on track type and national criteria. The intermediate gaps between the sleepers cause varying stiffness along the rail. The deformation of the rails due to the trains load on the wheels in combination with the movement cause a sleeper passing frequency that contributes to the resulting vibration. Furthermore, train axle/bogie dimensions can produce further vibration components of this mechanism. The dimensions discussed in Figure 2.10 and Table 2.4, are relevant to the parametric excitation. The respective dimension can be used to calculate the frequencies generated at the train speed v m/s using the following equation,

$$f = \frac{v}{l_n} \tag{2.12}$$

where l_n refers to the dimension considered (sleeper or axle/bogie spacing), in metres, which can be interpreted as the wavelength produced by the particular dimension. In this way, the parametric excitation components are related to the train speed.

Variation in contact force that produce excitation of vibration can arise due to other factors. Among these are singularities in the track (e.g. switches or other discontinuities), hanging sleepers where the ballast fails to provide full support, or differences in the stiffness of the supporting structure and subground. Moreover, acceleration, braking and variations in alignment between the two rails can cause dynamic forces that generate vibration. These are some further examples of the many factors that can induce vibration. Train induced ground vibration constitutes a rather complex dynamic system, and the modelling of such a system is limited by the parameters taken into account, as well as the available input data. This is something to keep in mind when setting up a prediction model, but also when interpreting measurement data.

2.3.3 Critical Velocities and Ground Vibration Boom

A phenomenon similar to a sonic boom can arise within ground-borne vibration, a so-called ground vibration boom, which is a sort of shock wave build up of the wave front. This occurs when a train is travelling close to, or at equal velocity as the propagation speed of Rayleigh waves in the immediate underlying subground, or the minimum phase velocity of bending waves in the rails [28]. The former being referred to as the critical wave speed and the latter critical track speed. Usually, the critical track speed is around 10 to 30 % higher than the Rayleigh wave speed at the site under consideration [28]. In very loose ground materials, the propagation speed of the Rayleigh wave is relatively low, and a high-speed train could be running at the critical wave speed (for information on wave speeds, see Section 2.1.1 and 2.2). If this is the case, a large increase in vibration amplitudes will arise. When a ground vibration boom occurs, the wave front propagates in a semi-cone shape from the front of the train, with the cone pointing in the direction of travel. Other phenomenon such as wave guiding can arise due to the geometry of the track and substructure, e.g. if the track has an embankment. This may cause lesser vibration outside of the embankment, but even higher ones inside of the bank where the wave front is guided [28]. The phenomenon of ground vibration boom was observed at a track site near Ledsgård in western Sweden, where a large deposit of very loose clay (muck) is situated below the track. With Rayleigh wave speeds down to 45 m/s, a relatively low train speed was sufficient to achieve the critical wave speed, circa 162 km/h. A tenfold increase in generated ground vibration was measured.

If the train approaches a velocity close to the critical track speed, an increase in the deformations of the rails occur, which could have a negative effect on train stability [28]. Based on Winkler beam theory of an infinite beam on top of an elastic foundation, the following expression can be used in order to calculate the critical track speed,

$$C_{min} = \left(\frac{4\alpha EI}{m_0^2} \right)^{1/4}, \tag{2.13}$$

where E is the Young's modulus of the rail material, I is the moment of inertia of the rail and m_0 is the mass per unit length of the rail [28]. α is in this expression referring to a proportionality coefficient of the equivalent Winkler elastic foundation, modelling the elastic ground. Further, as stated in [28], to approximate C_{min} for a particular site, α can be expressed as the elastic modulus of the ground material in question.

This phenomenon is an issue relevant to high-speed trains on soft ground materials, in particular. It may result in the need to lower train speeds for certain areas with soft soils underneath the track-structure. As train speeds are generally increasing world-wide, this phenomenon should be considered when planning a new railway or increasing speeds on an existing track. Yet again, it is of importance to determine the particular characteristics of the track and subground at the site of interest. For more information on ground vibration boom, see Chapter 9 in [28].

2.3.4 Information on Railway Track Design

The design of both the railway track and the supporting substructure influence how the generated vibration at the wheel/rail interface will be transmitted into the underlying subground (also referred to as subgrade). The main function of a railway track is to provide adequate support for static and dynamic loads in lateral, longitudinal and vertical directions. The underlying supporting structure should distribute the load induced by moving trains so that minimum pressure is applied to the subground. A favorable design of a railway system will attenuate some of the generated vibration, and the track system will usually exhibit a low-pass filter like response to excitation [2]. One can speak of an insertion loss for a certain railway system design, which can be utilized when predicting vibration from a railway. Insertion loss is defined as the ratio between the transmitted power with a certain track system in the transmission path, and transmitted power without the track system/isolation. There is a multitude of track designs which all vary in their resilience to excitation. The following paragraphs aims to present some common features of generic railway systems, briefly. For further reading on this topic, the following documents are recommended; [30], [9] and [29]. This section is to a large extent based on the information provided in these resources.

The so-called ballasted railway track is a track type commonly used worldwide. This track typically incorporates a set of two rails that are mounted in top of supporting concrete sleepers using rail fasteners, with a rail pad in between. The sleepers are resting on, and are embedded into ballast material, which in turn is supported by subballast resting on top of the subground, see Figure 2.14 and 2.15. The following paragraphs describe the separate components of this type of track design.

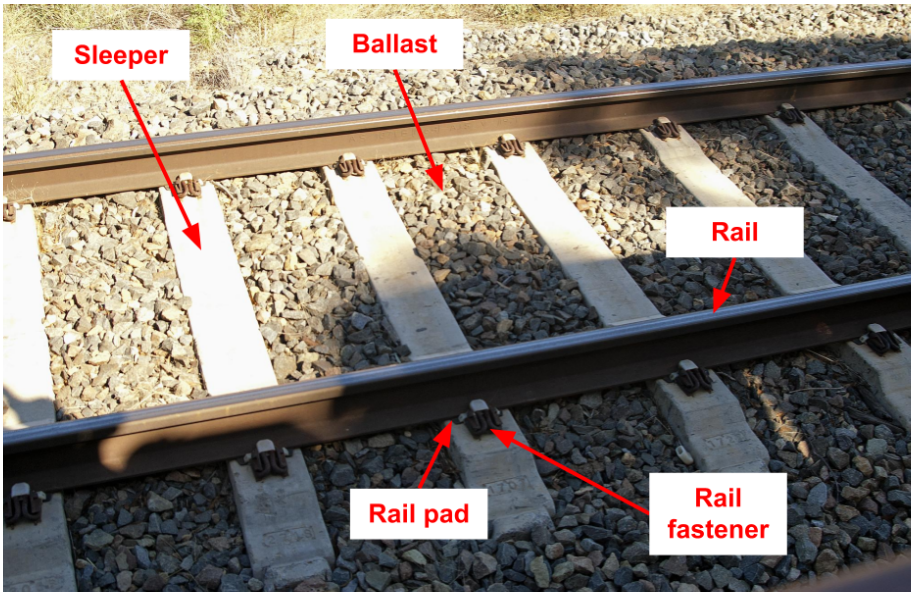

Figure 2.14: A picture of a typical ballasted railway track system with concrete mono-block sleepers (Main Southern railway line in New South Wales, Australia). Figure acquired from [27]. Note: Picture adapted with marked components.

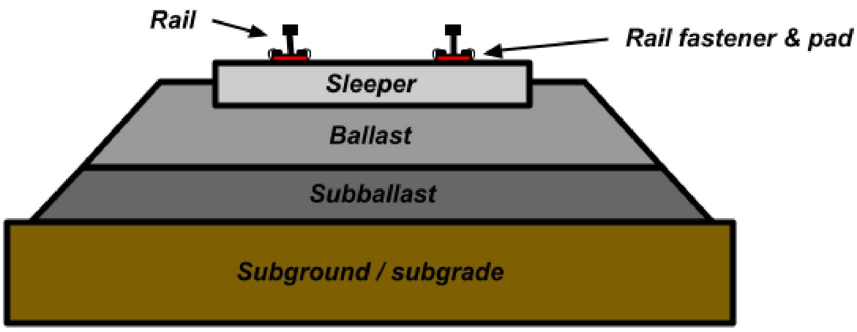

Figure 2.15: A schematic figure illustrating a typical supporting structure of a railway system.

The rails of a railway system are made of hardened steel, and can be manufactured to relatively high geometric tolerances. They should provide a smooth and precise track geometry that gives low variation in contact force between rail head and wheel tread. The rail is secured to the sleeper by means of a rail fastener. Between the rail and sleeper there is usually an elastomeric material, which acts as a damper for part of the structure-borne sound generated in the rails. Common materials for sleepers are either wood or concrete. A sleeper is usually semi-embedded into the ballast, and provides support and mounting points for the rails. They are evenly spaced along the track and are intended to distribute the load from the rails, and to increase the mechanical impedance of the track system as a whole. There are several types of sleepers in use world-wide, e.g. mono-block sleepers (seen in Figure 2.14) or twin-block sleepers, where each rail has its own set of sleepers.

The ballast material functions as a load distributor and shock absorber, but also as water drainage for the track system. Usually, ballast is made of a granular material, like coarse gravel. The ballast sits on top of the so-called subballast, which shares the same functions as the ballast, but is typically made of a material type with finer grain size. This can be a mixture of crushed graded rock and sand/gravel [30].

Finally, the track system is supported by the subground/subgrade. This is the point at which the track system is connected to the natural ground material present at the site. However, the subground can also constitute man-made consolidated materials to increase the subground stiffness. A track embankment can be constructed between the subballast and subground, if the material underneath the track structure is considered to be too soft. This construction basically raises the track and helps to decrease the pressure applied to the subground by means of load distribution over a larger area (note: according to ISO 14387 [2], energy transmitted into the subground from a graded or raised track system is to a large extent in the form of surface waves). An embankment can also help to better drain away rainwater from the track. For the case of a soft supporting ground material around the track, further types of stiffening measures can also be used, like pile driving in and around the supporting subground of the track. In some cases, a ballast-less track can be utilized in order to increase the precision of the track geometry and to achieve a more resilient track form with regards to vibration. A continuous concrete slab is then used in place of the ballast, which can be installed with higher track geometry tolerances. It increases the stiffness and distributes the load more evenly compared to a classic ballast track. This generally allows for higher train speeds and lower vibration around the track. More information on track systems can be read in [29] and [30].

2.3.5 A Few Words on Measurements of Railway Ground Vibration

Measurements of ground vibration generated by railway systems are of great importance since the complex engineering task of predicting vibration values, presumably need both calculations/simulations and measurements in order to draw valid conclusions, due to many factors of uncertainty. The measurement itself can produce erroneous data. For example, resonances within the measurement equipment can affect the frequency spectrum of the measured signals. Even so, there are standard procedures that should be implemented when measuring ground vibration.

Care should be taken so that the Signal-to-Noise-Ratio (SNR) between the ambient background vibration levels and the expected vibration levels from the source is sufficient. The transducers should be applicable for the targeted frequency range, which would be around 1 to 80 Hz for ground-borne vibration and 16 to 250 Hz for ground-borne noise (on soft ground materials, i.e. not rock materials). Measurement equipment should be calibrated according to international standards, see ISO 8041 [32]. An appropriate cut-off frequency of the anti-aliasing filter should be set when using a digital data acquisition system. Moreover, the installation of the transducers should allow for a faithful representation of the actual vibration source. Secure placement of the transducer is needed, preferably with no inherent resonances of the mounting system occurring within the same frequency range as the measurement target range. The standard ISO 5348 provides guidance on mounting of accelerometers [31].

Due to possible variations in the ground layers at the measurement site, it is recommended to conduct multiple measurements at separate points. When measuring vibration from a railway track system, ISO 14387 [2] recommends measurements at multiple points separated along a perpendicular line from the track. This line measurement should be repeated at least twice, with the perpendicular lines being 25 metre apart. For further information on measurements of ground vibration from railway systems is provided in the separate parts of ISO 14387 [2].

2.4 Human Response to Low Frequency Vibration, Weighting Filters and Building Response

Humans can experience noise and vibration both through physical movements of the body and via pressure variations arriving at the ear drum. The standard ISO 2631 [33] provides guidance on how to evaluate human exposure of whole-body vibration, and presents information on measurements and post-measurement processing of the acquired data. Whole-body vibration depends on several factors and can be difficult to quantify. To a certain extent, perception of noise and vibration is even subjective, but the aim of the standard is to enable rational methods of evaluating whole-body vibration perception. In Figure 2.16, the human perception threshold over frequency is presented. The graph is based on ISO 2631 [33]. It can be seen that humans tend to have a higher sensitivity to vibration in the range of 8 to 80 Hz, than compared to lower frequencies (1 to 8 Hz).

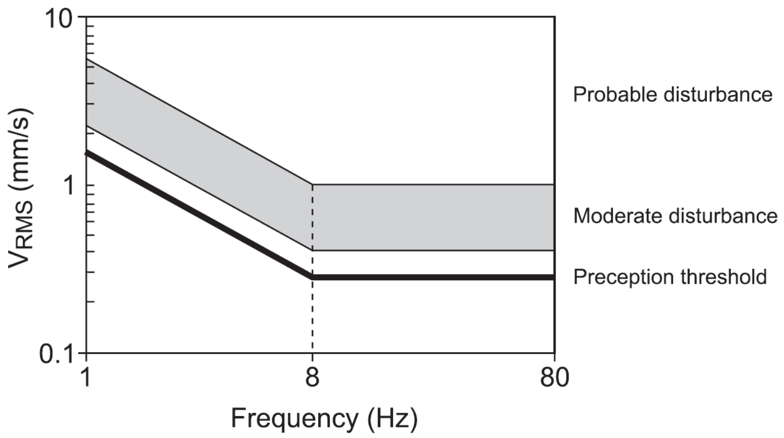

Figure 2.16: Human threshold for perception of vibration, along with levels of disturbance. Figure acquired from [34].

Frequency weighting is done in order to relate vibration levels to the experience of a human receiver. This is equivalent to weighting of sound pressure levels to evaluate how sound is perceived by humans, like for example applying the A-weighting filter. The weighing filters are based on empirical studies of human vibration exposure. ISO 2631 [33] presents several weighting filters that can be applied to vibration level spectra depending on the studied case. Weighting using the standard can be done in order to evaluate the effects of vibration on humans related to health, perception, motion sickness and comfort. The frequency ranges considered in this standard are 1 to 80 Hz for health, comfort and perception related issues, and 0.1 to 0.5 Hz for motion sickness evaluation. However, the weighting filters are applicable up to the 400 Hz one third octave band.

Further, there are three main positions or axes of the human body which is used for quantifying human vibration perception; seated, standing and recumbent position. The weighting categories for perception, health etcetera, plus the defined axes of the human body are used to determine the particular frequency weighting curve to be applied to the vibration spectrum. According to the standard, the vibration spectrum should be presented as the Root-Mean-Square (RMS) value of the acceleration in all three orthogonal directions, which could also be represented as velocities. It should be noted that the metrics used within these types of measurements and post-processing differs between some national standards. It is therefore of high importance to declare precisely what type of value that is computed and presented. It is crucial to state if it is a peak or RMS level, or if the spectrum presents a momentary value or an average over time, as well as the quantity type; acceleration, velocity or displacement.

A building can in worst case amplify vibration transmitted into the structure. This can happen at e.g. long floor spans. To draw conclusions on the effect of vibration inside of a building due to a predicted vibration spectrum at the building foundation, a frequency response function of the building itself is needed. This function will include all of the transmission effects in the structure (when studying structure-borne sound, radiation effects inside the building would have to be accounted for). According to ISO 14837 [2], the frequency range of interest which incorporates both whole-body vibration and audible noise within buildings is approximately 1 to 250 Hz. Further, the standard states that frequencies below 100 Hz are usually the most dominant when studying the building response. Also, it is very rare for building damage to occur as a result of vibration from man-made sources. However, ISO 14837 [2] declares that most damage will most likely occur within the frequency range of 1 to 150 Hz.

3
The High-Speed 2 Prediction Model

This section presents the empirical High-Speed 2 noise and vibration prediction model. The chapter is initiated with a short section on ground vibration prediction models in general, with some examples of other models in use today. Further, the chapter includes an in-depth description of the model as documented in the reports and papers [5], [6] and [7]. The HS2 model, as described in Section 3.2 (and in the model documents), was implemented into a Matlab script during the thesis.

3.1 Prediction Models for Railway Induced Ground-Borne Noise and Vibration

Due to the complex nature of ground-borne noise and vibration in an engineering context, companies often perform initial predictions using empirical and/or numerical models. To enable computation of the complete system, the model must incorporate parameters describing the source, propagation and receiver. There are a lot of possible implementations and the quality of the predictions depend on the backbone theory incorporated, as well as the input data used. The type of model used can also depend on the stage of the assessment, i.e. if only a rudimentary indicative model is sufficient, or if more detailed models should be utilized. ISO 14837 [2] provides information on parameters that should be taken into account when using a ground vibration prediction model, and also highlights important aspects when developing and/or validating the models. According to the standard, it is useful to divide prediction models into three categories, with complexity that reflect the stage at which the vibration assessment/project currently is at. These categories are;

1. **Scoping model:** A model that is used in the beginning of a ground vibration assessment. It uses a set of relatively few generic input parameters to enable decisions on potential sites where noise and vibration could become an issue. The model should approximate the overall worst case levels of the noise and vibration. Naturally, in the beginning of a project incorporation vibration assessment, limited data and information useful to ground vibration prediction is available. Scoping models use only a few basic parameters, such as rail system type, distance between source & receiver, generic ground conditions (soft, medium or hard) and type of receiving building.

2. **Environmental Assessment Model:** Used to compute more accurate predictions when more detailed information on the source, transmission path and receiver is known. Possible mitigation measures can also be included in the model. If a new railway system is under development, this model should provide a basis for preliminary design.

3. **Detailed Design Model:** This model should provide a more accurate prediction as the quality of the input parameters are excepted to be higher at this stage. The computations should provide information to base detailed design and potential mitigation plans on.

Annex A of ISO 14837 [2] presents a list of parameters that can be considered depending on the demand of model accuracy and the indented use of the results. It provides a good insight into what key parameters that affect generation, transmission and immission of ground-borne vibration from railway systems.

Regarding the actual calculation methods used within prediction models, there are three main categories, namely, empirical, numerical and algebraic models. Obviously, algebraic ones are typically rudimentary, and are sometimes inconvenient to use. Empirical and numerical models, or a combination of the two are often used for ground vibration prediction today. However, there is no standardized prediction model in use on a global scale, and several noise and vibration experts have developed their own models based on experience. There are however a few models that have been developed and utilized successfully within multiple projects. Among these are the numerical ground vibration prediction model of Banedanmark [35], and the semi-empirical model of the Norwegian Geotechnical Institute (NGI) [36]. Further, the previously mentioned empirical prediction models of HS1 and HS2 [5] and [6] have been used at multiple occasions, globally.

Empirical models have the advantage of averaging over a multitude of separate in-situ measurement cases (as for the HS1 and HS2 model which are based on over 3000 measurements). This means that variability of different parameters are inherently included in the reference data used. Numerical models such as the Finite Element Method, Finite Difference Method or Boundary Element Method, can be utilized to achieve a relatively detailed model of for example a specific vibration generating mechanism or response of building, but requires accurate input data as well as correct boundary conditions. Depending on the case and aim of the assessment, it can be advantageous to use multiple model types for vibration prediction.

3.2 Description of the High-Speed 2 Prediction Model

A general introduction to the HS1 and HS2 projects was presented in Section 1.1. The following section presents the calculation method of the HS2 model, in-depth.

The ground vibration prediction model developed in the HS2 project is an extension of the empirical HS1 model, enabling extrapolation of vibration values of lower train speeds to higher ones for a proposed train (up to 360 km/h), or from higher to lower. This is done by utilizing a vibration spectrum of a reference train as a baseline source, and applying appropriate corrections to produce a predicted spectrum for the proposed train. The model can be used to predict vibration levels at a receiver position R metres from the nearest rail of the track, and includes calculation procedures for both surface and tunnel running trains. The model takes into account the source (train/track dimensions), insertion loss of the track system and the propagation through the surrounding subground. The propagation correction is performed using coefficients and a formula that accounts for both the geometrical attenuation and material damping that occur in the transmission path to the receiver position, for a certain generic ground material type. Furthermore, together with building response functions, weighting filters and time averaging due to an expected train flow, noise and vibration levels can be approximated inside of dwellings and other buildings in the vicinity of the railway. According to [8], the model's 95 % confidence interval for predicted ground-borne noise and vibration levels are within ± 8 dB.

Since HS1 and HS2 are based on measurement data, there are several parameters defined within the model that are used as baseline reference values. From the thousands of measurements conducted in the HS1 project, data of vibration propagation on several types of generic ground materials (referred to as lithology types in the model) are documented. These materials are sand, sand & clay mixture, chalk and clay. Furthermore, the reference source terms are defined for two train types, namely Eurostar 373 / e300 (high-speed train) and British Rail Class 322 (passenger train, here on referred to as CL322). Reference spectra of the Eurostar train has been derived for sand, sand & clay mixture and chalk, and CL322 for clay lithology. Insertion losses for three track system types are defined, as well as a generic function describing the so-called effective roughness (roughness excitation of rail/wheel), which together with the parametric excitation is used to describe the two excitation mechanisms of the reference and proposed train. All of the reference data mentioned are documented in tables found in the two published HS2 documents [5] and [6] (also available in Appendix A). These documents include a description of the model work flow, as well as formulas for calculations in each step, see Figure 3.1. In this thesis project, the main focus is surface running trains. Therefore, the following explanation of the calculation procedure will be of a surface train case. Further, low-frequent ground-borne vibration is the main target. This is the reason for only conducting the steps of the left wing of the flowchart after propagation correction (the right wing would be used to compute predictions for structure-borne noise).

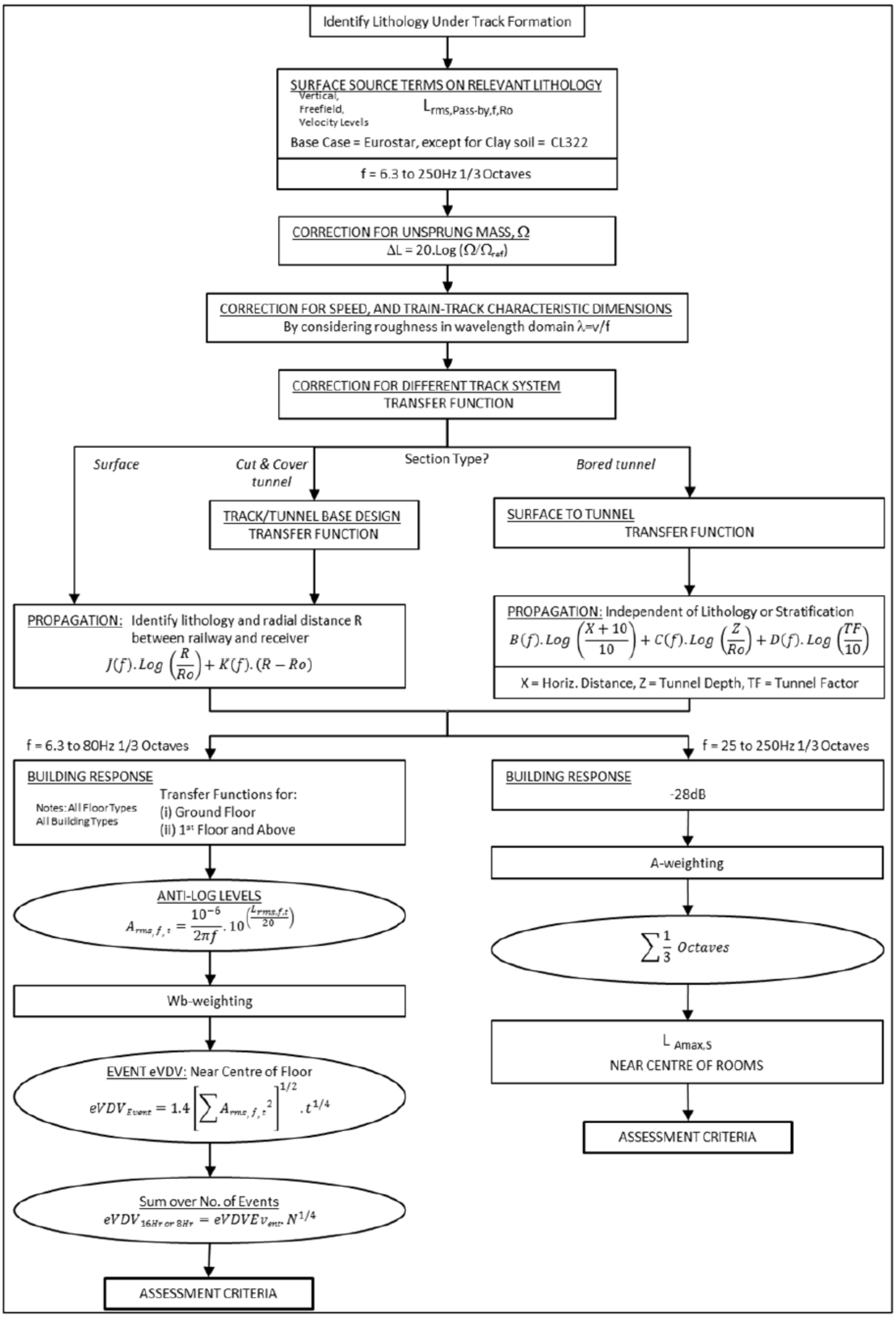

Figure 3.1: Flowchart summary of the HS2 prediction model. Figure acquired from [5].

3.2.1 Step 1: Identify Lithology Under Track Formation

When conducting calculations using the HS2 model, the first step is to identify the geological conditions at the site of the investigation. The objective is to determine under which of the four different generic material types of the model that the studied case is most correlated to, with regards to material properties.

Note: the HS2 documents do not present any criteria or procedure for actually determining the properties at the site. Possibly, a geological study with seismic measurements could be performed in order to determine the shear wave speed of e.g. the top soil layer. The calculated wave speed can then be used together with tables of material properties (like Table 2.3 presented in the Theory section of this report), to acquire a rough estimate of the major component of the ground layer profile. This should however be done with caution, since material properties of soils can vary drastically, for example if the soil has a high water saturation.

3.2.2 Step 2: Surface Source Terms on Relevant Lithology

In the second step, the reference source spectrum for the determined lithology is chosen. The source terms are measurements of the vertical component of the soil particle movement at 10 metres from the nearest rail, presented as the RMS of the free-field vibration velocity level in dB (reference value 10^{-6} mm/s), in one third octave bands from 6.3 to 250 Hz (centre frequency). The reference values are spectra calculated from measurement data evaluated over the train passage period. The reference source terms are defined in Table 2, Annex D1 of [5] (also available in Appendix A, Table A.1 of this report), and are derived from measurements conducted on good quality ballast tracks in France and the UK [5]. As mentioned previously, the source spectra of the Eurostar train are used as the reference for all ground material types within the model except for clay, where the CL322 vibration spectrum is used instead. Figure 3.2 present the reference source terms included in the HS2 model.

Note: no specific information on how to evaluate the train passage time in the measurement time signals is presented in the HS2 documents.

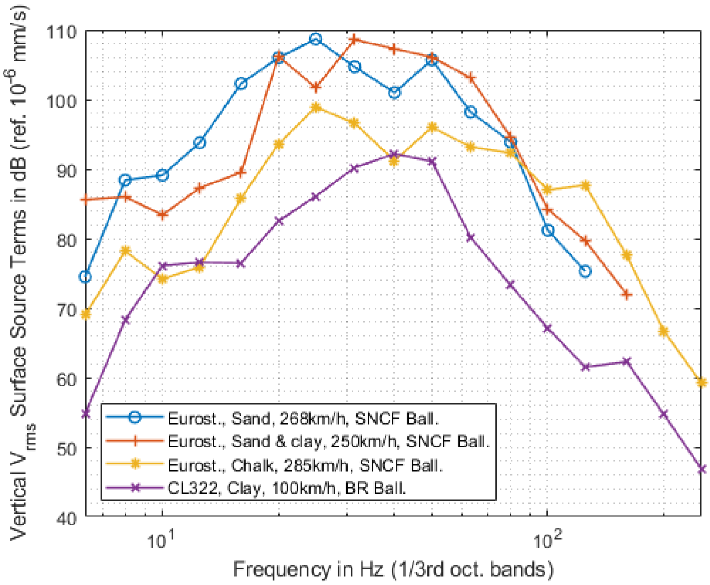

Figure 3.2: The HS2 reference source terms. Data from Table 2, Annex D1 [5] (also available in Appendix A). SNCF ball. refers to French standard ballast track system, and BR ball. to British standard ballast track system.

3.2.3 Step 3: Correction for Unsprung Mass

In the third step, a level correction factor, denoted ΔL, for the unsprung masses (in kilograms) of the proposed train and reference train is derived using the following expression,

$$\Delta L = 20 \log_{10} \left(\frac{\Omega}{\Omega_{ref}} \right), \tag{3.1}$$

where Ω is the average unsprung mass of the proposed train, and Ω_{ref} is the average unsprung mass of the reference train.

The calculated delta is then added to the proposed train's source spectrum. This will result in a shift of the complete spectrum line by a certain level in dB.

3.2.4 Step 4: Correction for Speed and Train-Track Characteristic Dimensions

In this step, characteristic dimensions of the track and train are used to define the parametric excitation caused by the dynamic wheel and rail interaction, the passing frequencies of e.g. the sleepers when the train is running. Further, a roughness spectrum is also utilized to account for the wheel and rail roughness excitation.

A generic roughness profile (roughness amplitude per wavelength) was derived from a known rail roughness that is representative of good quality ballast track [5]. This roughness spectrum is based on data from efforts made in a Crossrail noise and vibration assessment [37], and from measurements conducted with corrugation analysis trolley at Steventon, England [38]. The spectrum includes data of roughness amplitude for wavelengths of 0.01 to 25 meters, and can be viewed in Figure 3.3. According to the HS2 documents, roughness levels for each source term spectrum and for the different track types were not available. Instead, this generic roughness curve has been adopted in the HS2 model [5].

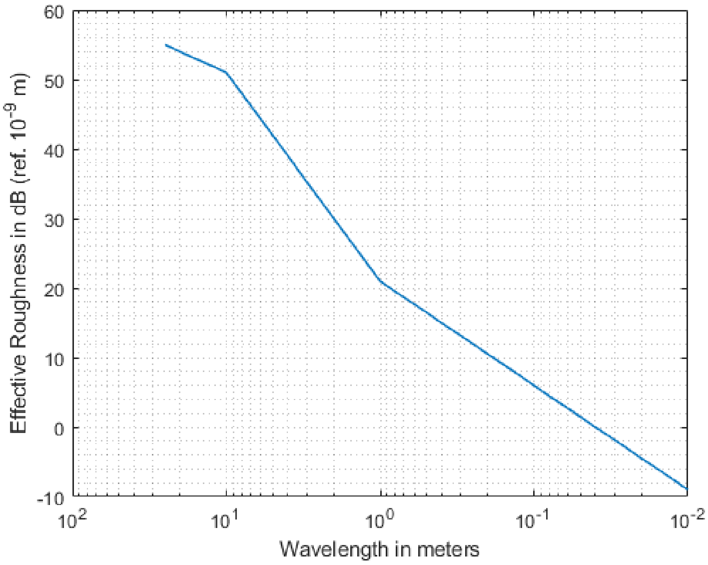

Figure 3.3: The given effective roughness spectrum of the HS2 prediction model, data from [5]. Data table also available in Appendix A.

The generic roughness profile is used as the reference spectrum for wheel rail roughness excitation for both the reference train and proposed train. The next substep is to utilize parabolic functions that describe the parametric excitation of the reference train and proposed train respectively. These functions are superimposed onto the generic roughness spectrum to form a spectrum representing the parametric and roughness excitation, one for each train. The parabolic functions denoted L_K, describe the contribution in vibration level from the passing frequencies of the K^{th} sleeper or axle distance, etcetera [7]. The relevant input dimensions of the track and train adopted by the HS2 model are defined in ISO 14837 [2]. They are also presented in Section 2.3.1 of this report. The following equation is utilized to calculate the parabolic functions (one function per relevant track-train dimension),

$$L_K(\lambda) = R(\delta_K) + A - \left(\frac{\log_{10}\lambda - \log_{10}\delta_K}{B}\right)^2, \tag{3.2}$$

where λ is the wavelength in metres, δ_K is the K^{th} sleeper or axle spacing and $R(\delta_k)$ is the amplitude of the generic effective roughness term at the wavelength produced by the K^{th} sleeper or axle spacing [7]. A and B are constants describing the shape of the parabolic terms, namely the amplitude and width. These can be tuned to provide a better fit to measurement data. In Figure 3.4 below, the generic effective roughness curve and the parabolic functions of an example train are plotted.

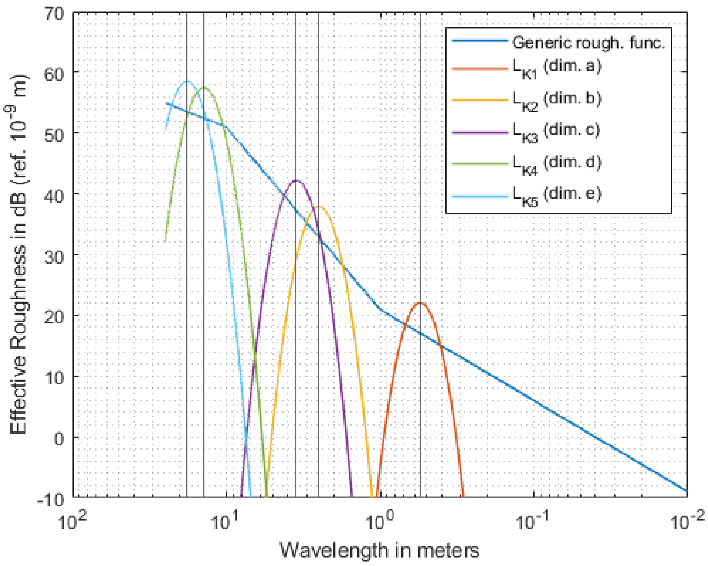

Figure 3.4: The generic roughness curve and parabolic functions representing the contribution by the different relevant track-train dimensions (the calculated L_K's).

In Figure 3.4, the vertical lines represent the centre wavelength produced by the respective track-train dimension, which coincide with the vertex of the parabolas. The parabolic function L_{K1} correspond to the sleeper spacing a, and L_{K2}, L_{K3}, L_{K4}, L_{K5}, to axle dimensions b, c, d and e respectively, as defined in Figure 2.10, based on ISO 14837 [2].

By superimposing the calculated L_K functions with the generic effective roughness curve, a train-specific effective roughness, denoted R_{eff} is obtained. This is done for both the reference train and for the proposed train. The following expression is utilized, as stated in [7],

$$R_{\text{eff}}(\lambda) = 10 \log_{10} \left(10^{R(\lambda)/10} + \sum_K 10^{L_K(\lambda)/10} \right). \tag{3.3}$$

In Figure 3.5 below, an example spectrum of R_{eff} is presented.

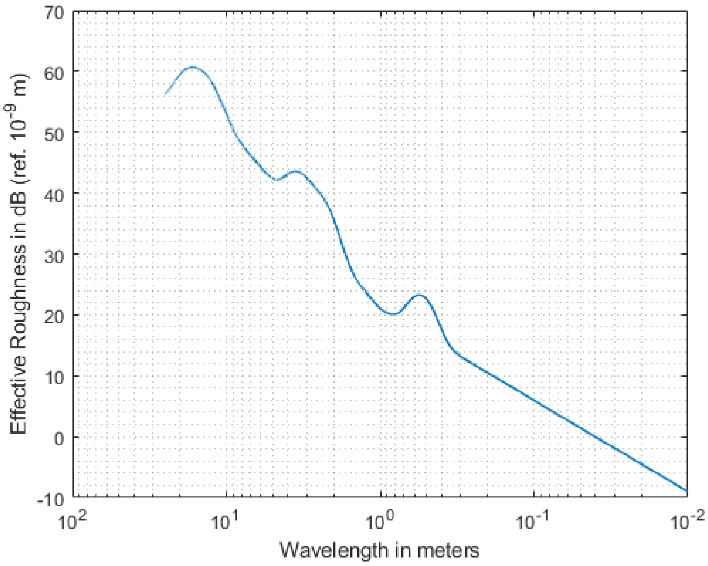

Figure 3.5: The train-specific effective roughness spectrum over wavelength.

Then, by utilizing the relationship presented in Equation 2.12 ($f = v/\lambda$), the effective roughness spectra are related to their respective train speeds. The reference train travels at speed v_1 and the proposed train at speed v_2. Figure 3.6 presents an example spectrum of R_{eff} related to the train speed, amplitude over frequency.

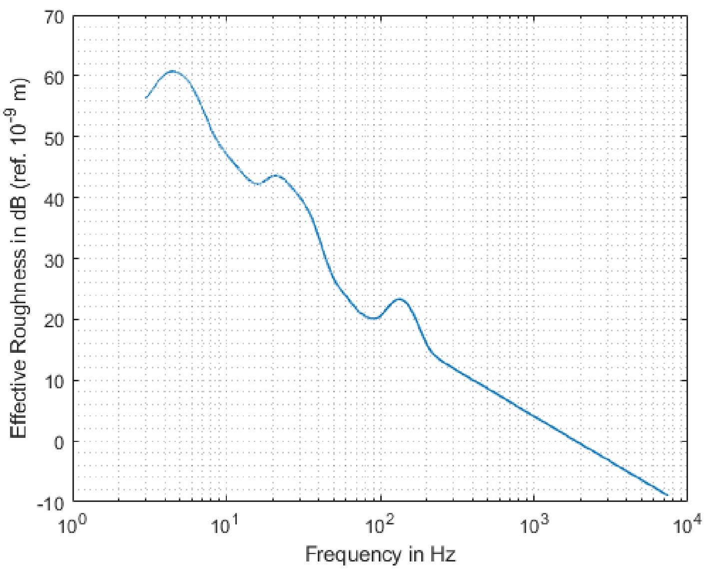

Figure 3.6: The train-specific effective roughness spectrum over frequency (related to the train speed).

Once a spectrum as presented in Figure 3.6 is calculated for both trains, the difference at the centre frequency of each one third octave band is calculated (proposed train spectrum subtracted by the reference train spectrum in each band). To correct the reference spectrum and obtain an estimation of the proposed train spectrum, the calculated delta in each band is added to the unsprung mass corrected reference spectrum.

3.2.5 Step 5: Correction for Different Track System

If the reference train and proposed train use different track systems, the insertion losses of the reference track system and proposed track system are utilized to calculate a delta between them. This is done by subtracting the reference train's insertion loss with the proposed train's insertion loss. Once calculated, the delta is then subtracted with the unsprung mass and speed corrected spectrum of the proposed train, to correct for the difference in insertion loss between the track systems. The insertion loss is in the model documents defined as the change in vibration level at 10 metres from the nearest rail of the track, if one track system is replaced with another. The insertion loss levels are calculated with reference to a hypothetically "highly" stiff reference track, according to the HS2 documents.

In the document [6], there are insertion losses defined for three different track systems, namely SNCF ballast (the French National Railway Company's standard ballast track), BR ballast (the British Rail company's standard ballast track) and a so-called "base case track". The HS2 documents states that the base case track for surface sections is a resilient slab track that is optimised to provide track stiffness and vibration isolation performance similar to ballast track. No additional information on these track systems are given in [5] or [6]. The insertion losses of the different systems are presented in Figure 3.7 below. The data is presented in Table 3, Annex D1 [6] (also available in Appendix A, Table A.2 of this report).

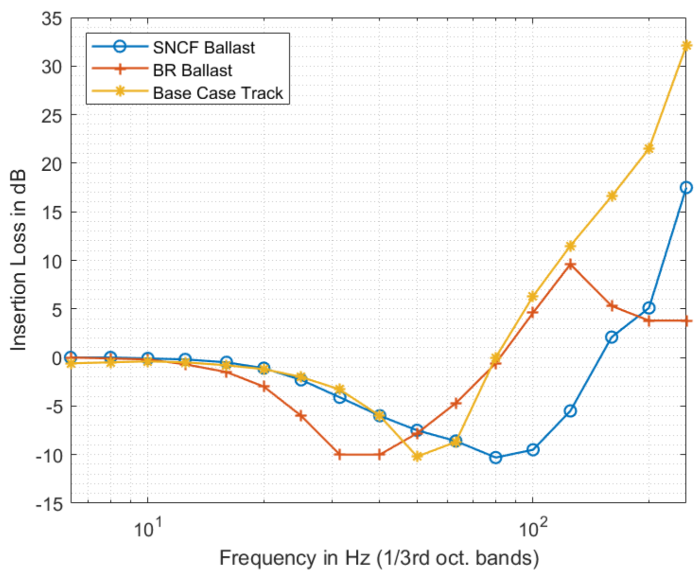

Figure 3.7: The HS2 insertion losses plotted over frequency (the track systems are here on referred to as SNCF, BR and BCT respectively).

Before proceeding with further calculations, the section type for the proposed train must be determined. i.e. if the proposed train will run on a track at surface level, cut & cover tunnel or a bored tunnel. There are separate calculation methods for the different section types, as can be seen in Figure 3.1. This thesis focuses on low-frequent vibration from surface running trains, hence the following steps will describe calculations for this case.

3.2.6 Step 6: Propagation Correction

In step 6 the vibration propagation from the track system to a receiver position at a radial distance R metres from the nearest rail of the track is accounted for. The formula for propagation correction accounts for the geometrical attenuation and material damping that occurs in the chosen ground material over the distance R. The propagation model for surface running trains has been derived from vibration analysis of train passage measurements by a variety of trains in the UK, France and Germany, on ballasted track. According to the model document [5], the main subground layer governs the attenuation between source and receiver.

The correction is calculated using the equation presented for this step in the flowchart, together with a set of propagation coefficients, J and K, for the different lithology types defined in the HS2 model. The propagation correction, here referred to as $P_{\text{corr.}}$ is defined as;

$$P_{\text{corr.}} = J(f)\log_{10}\left(\frac{R}{10}\right) + K(f)(R-10), \tag{3.4}$$

where J and K are the ground material coefficients in each one third octave band, which are defined in Table 7 of Annex D1 in [5], and are also presented in Table A.4, Appendix A of this report.

When $P_{corr.}$ is calculated, it is then added to the unsprung mass, speed/track-train and insertion loss corrected spectrum of the proposed train. Now, vibration levels at R metres from the railway track is obtained. Depending on the demand of the calculations, the subsequent steps of the model can be utilized to obtain weighted vibration levels and/or noise levels inside of a building.

3.2.7 Step 7: Building Response

In step seven, building transfer functions are used to translate the vibration level values on the ground surface at distance R metres (at the soil surface outside of the building foundation), to vibration levels excited within the building at the floor level of interest. For low frequent vibration it is usually the vibration level at the middle of a floor span that is of interest. This can be relevant for comparing predicted values to limiting values set for a particular building or area.

3.2.8 Step 8: Anti-log Levels

Prior to applying a weighting filter to the calculated values, anti-log levels are calculated from the spectrum computed after accounting for the building response function. To calculate a so-called estimated Vibration Dose Value (eVDV) in the subsequent steps, the RMS of the acceleration is used. Since the L_{rms} levels are particle velocity levels, the anti-log formula contains an integration in frequency domain, by multiplication of $2\pi f$, to obtain acceleration. The anti-log acceleration values, denoted $A_{rms,f,t}$, are calculated using the following formula,

$$A_{rms,f,t} = 2\pi f 10^{-6} \left(\frac{L_{rms,f,t}}{20} \right). \tag{3.5}$$

Note: the anti-log formula presented in [5] is seemingly incorrect if the goal is to compute the acceleration, since that formula uses a division of $2\pi f$ in frequency domain, which would produce displacement if L_{rms} are velocity values (see anti-log level formula in Figure 3.1).

3.2.9 Step 9: Weighting

Depending on the aim of the predictions, the appropriate frequency weighting filter is applied to the acceleration values in this step. For more information on weighting, see Section 2.4 of this report.

3.2.10 Step 10: Event eVDV

In step 10, the event eVDV is calculated for a train passage near the centre of the floor span in question. The following equation is used to calculate $eVDV_{event}$,

$$eVDV_{event} = 1.4 \left[\sum A_{rms,f,t}^{\,2} \right]^{1/2} t^{1/4}, \tag{3.6}$$

where $A_{rms,f,t}$ is the acceleration value near the centre of the floor span and t is the train passage period.

3.2.11 Step 11: Sum over Number of Events

In step 11, the calculated $eVDV$ value is summed over the number of events occurring (the number of trains passing by) during either 8 or 16 hours. This is done using the following equation,

$$eVDV_{16Hror8Hr} = eVDV_{event} N^{1/4}, \tag{3.7}$$

where N is the number of events occurring during the selected time frame, 8 or 16 hours. The number of events could be based on information on expected train flows for the particular railway line (during night and/or day). Other information about the train operations would be needed to approximate the $eVDV_{16Hr or 8Hr}$ value, e.g. data of train types, speeds, length of train sets and so on (this would be used to compute the predicted vibration per event).

3.2.12 Step 12: Assessment criteria

In the last step, an assessment criteria can be determined, and measures can then be taken accordingly. Depending on the computed vibration dose value and the limiting values for the building in question, it can be decided if the vibration inside of the building is determined sufficiently low, or if mitigation measures should be implemented in order to reduce the excited vibrations.

4

Train Passage Measurement and Data Processing

This chapter describes the train passage measurement conducted by Efterklang, of which the data was acquired for use within this thesis. The methodology of the measurement data processing is presented in the last section of this chapter.

4.1 Description of Train Passage Measurement

Measurement data of train passages were obtained during the thesis, supplied by Efterklang - part of AFRY. The measurement was conducted on the 30$^{\text{th}}$ of June 2009 on behalf of a Client, at a site along the Western Main Line, near Greby, Skövde in Sweden (see Figure 4.1). It should be noted that railways in Sweden use left-hand traffic, meaning that traffic on the western track of the Western Main Line is going from Skövde towards Töreboda. Data sets along with a measurement report draft and some other miscellaneous information were acquired. This section aims to describe the conducted measurements, as documented in the measurement report draft and other documents obtained from Efterklang.

Figure 4.1: Measurement location near Greby in Skövde, Sweden, coordinates: 58°32’02.6"N 13°58’40.4"E. Screenshots from satellite pictures taken in Google Maps.

The goal of the measurement was to document ground vibration from a variety of passing trains for comparison with calculations. Apart from a multitude of different train types that passed during the measurement, a Regina train operated by the Client was used during measurement of several passages, under controlled circumstances, i.e. that the speed of the train was known during the passages. The measurement included measuring the vertical component of the soil particle acceleration, and were documented as raw time signals. The acceleration time signals were provided in m/s^2. The conversion by each transducer's sensitivity (sensitivity of accelerometers are usually given in $mV/(m/s^2)$ or mV/g) was done either in the data acquisition system or afterwards prior to saving the data in the provided mat files. A total of 16 transducers and 13 measurement positions were used (mostly ICP eccelerometers from the manufacturer PCB, but also three seismic accelerometers from Wilcoxon). 28 seperate train passages of different types were measured, and six of the passages were with the Regina train at know train speed. The data acquisition system used was a PAK Mobile MKII from Müller-BBM. All equipment was calibrated to satisfy criterion of ISO/IEC 17025. The measured frequency range was 0.2 to 200 Hz, although the data was high-pass filtered so that the amplitude of the signal is reduced by 50 % at 0.5 Hz. This was done due to a disturbance at 0.25 Hz. The sample rate used in the data acquisition system was 512 Hz.

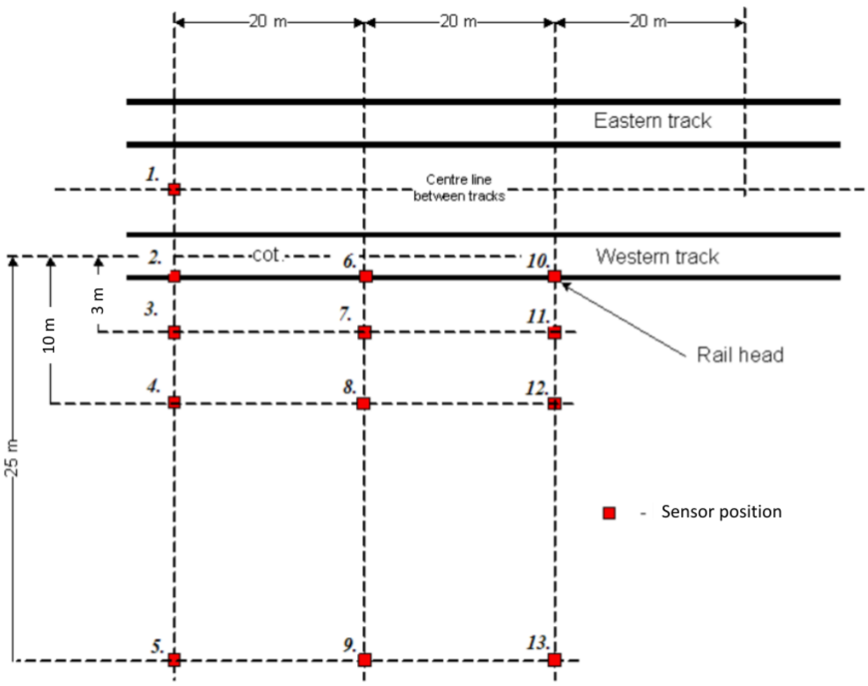

Figure 4.2: Transducer positions used during the measurement. Positions 5, 9 and 13 were equipped with two transducers per positions (one ICP accelerometer and one seismic accelerometer).

During the measurements, there were three types of transducer placements. Position 1 was an accelerometer fixed on a small square concrete slab recessed into the ballast between the eastern and western tracks, with sand between the slab and ballast material. At positions 2, 6 and 10 the accelerometers were fastened onto the underside of the rail using glue. Position 3, 7 and 11's accelerometers were also mounted onto a recessed concrete slab with sand into the ground. Lastly, position 4, 5, 8, 9, 12 and 13 were all glued onto a steel ground spike, secured into the soil. See Figure 4.3 for examples of the different transducer mountings. Note:

during data processing of the measurement data one should be aware of possible resonances occurring due to transducer mounting. Further, during the measurements, some of the sensors exhibited overloading, rendering some of the time data unusable.

Figure 4.3: Examples of sensor mountings used during the measurement. Example (a) - transducer on concrete slab recessed into the ground material, (b) - transducer mounted on the underside of the rail, (c) - transducer on concrete slab recessed into the ballast material and (d) - transducer on a ground steel spike.

No information on the prevailing geological conditions at the site during the measurement was obtained. Therefore, a geological map developed by the Geological Survey of Sweden was utilized to determine the generic ground properties at the site [21]. One should keep in mind that the map is based on sampling, and only provides some general information on the prevailing conditions. Therefore, the conditions declared by the geological map should be taken with a grain of salt, and viewed as a potential factor of uncertainty. According to the geological map, the ground material at the site is glacial clay over a bedrock of granite at approximately 3 to 5 metres depth (here one should be aware of possible resonances in the ground layer profile due to the relatively shallow depth to bedrock). According to the Geological Survey of Sweden, glacial clay is a fine-grained soil type deposited during the melting off the last icecap covering this part of the land [39]. According to [40], glacial clay is to a large extent composed of fine-grain clay particles with high plasticity. It has strong inherent cohesion forces between the grains and a very low amount of organic matter inside. Glacial clay may also hold sand and stone particles, sporadically. The load carrying capacity is stated to be varying from very high to very low depending on the current and past geological conditions, as well as loading history.

The data from this measurement was then utilized to compute the vibration levels using Fourier analysis of the time signals. The methodology for the measurement data processing is descried in Section 4.2.

4.2 Measurement Data Processing in Matlab

To enable comparison of predicted vibration levels of the HS2 model with measured data of train passages, the frequency spectra of the acquired measurement time signals needed to be computed for the relevant one third octave bands (6.3 to 250 Hz). The methodology for the measurement data processing done in Matlab is summarized in the following paragraphs. The core of the script is based on example code for Fourier analysis of time signals presented in Matlab's Fast Fourier transform documentation [41].

The first step in the data processing was to load one of the mat-files with the 16 channels of raw acceleration time data. The sampling frequency f_s was set to 512 Hz and the sampling period T (total signal length in seconds) was calculated by the following formula;

$$T = \frac{1}{f_s}. \tag{4.1}$$

In order to plot the time signal, a time vector t was computed using;

$$t = (0 : L - 1)T, \tag{4.2}$$

where L refers to the total number of discrete samples in the signal. Also, a frequency vector f was calculated by;

$$f = fs(0 : (L/2))/L. \tag{4.3}$$

Once the time signal was plotted, the actual train passage could be identified due the large increase in vibration from the noise floor during a passage. The subsequent step was to cut out only the relevant part of the signal for frequency spectrum analysis. However, the increase in acceleration amplitude from noise floor was typically gradual, meaning that it was difficult to determine at exactly which time instance the train passage "begins" and "ends". The HS2 documents state that the source spectra are derived from measurements of train passages that are evaluated over the train passage period. However, the documents do not describe how this evaluation was done. Therefore, a procedure of cutting each time signal was decided upon, in order to process the different time signals in the same way. The signals were cut so that roughly 1/3$^{\text{rd}}$ of the time signal is prior to passage, 1/3$^{\text{rd}}$ during passage and 1/3$^{\text{rd}}$ after passage. Using this procedure, the complete train passage remains within the time signal, yet the signal is drastically shortened. Potential differences in data processing between this thesis and the processing used for deriving the HS2 reference spectra have to be viewed as a potential source of error. As an example of time signal cutting performed for all measurement signals processed in this thesis, see Figure 4.4.

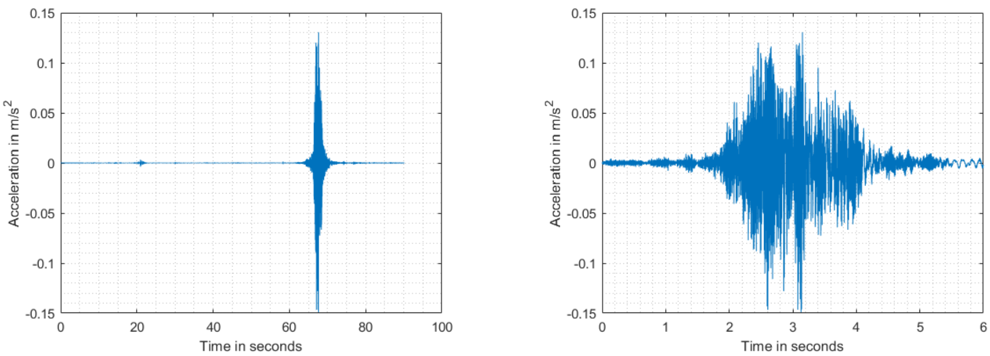

(a) Uncut time signal.

(b) Cut time signal.

Figure 4.4: Example of a time signal from a train passage at 250 km/h, transducer positioned 25 metres from the centre-line between the rails of the western track.

Due to the type of signal, transient signals with very low ambient vibration noise floor, it was decided to use a uniform window before conducting the Fourier transform. As the next step in the processing, the Fast Fourier Transform was performed on the time signal. The single-sided power spectrum was calculated by first dividing the double-sided spectrum with the number of samples, then splitting the double-sided spectrum at DC, and multiplying the single-sided spectrum by two (in order to maintain the correct energy of the spectrum). To compute the velocity spectrum, a derivation of the acceleration frequency components was performed in the frequency domain by dividing each component by $j\omega$ ($\omega = 2\pi f$). Also, the RMS value of each sinusoidal component was calculated by dividing them by $\sqrt{2}$. The levels were then calculated using the following expression;

$$X_{dB} = 20 \log_{10} \left(\frac{|X|}{10^{-9}} \right), \tag{4.4}$$

where X refers to the computed frequency spectrum. The reference value for velocity levels is 10^{-9} m/s.

As the last step, the narrow-band velocity levels were summed into their respective one third octave band using the equation;

$$L_{u,tot} = 10\log_{10}\left(10^{L_{u1}/10} + 10^{L_{u2}/10}\right), \tag{4.5}$$

where $L_{u,tot}$ is the total velocity level of the particular one third octave band and the L_{u1} is the level of the first frequency in the band, L_{u2} is the second frequency and so on. This was done for all one third octave bands from 1.25 to 250 Hz (centre frequency). This frequency range was computed in order to enable comparison of the measurement with predicted values of the HS2 model, and also to plot the measurement's frequencies below the HS2 range. However, the frequency band of 250 Hz was set to Not-a-Number due to lack of measurement data in this band (as mentioned, the measurement frequency range was from 0.2 to 200 Hz).

The to produce an averaged spectrum of one train passage for comparison with the HS2 model, the complete calculation procedure presented in this section was repeated for all measurement positions relevant for the subsequent comparison. One-third octave band spectra were therefore computed for all relevant positions. For each measured speed of the Regina train there were several accelerometer positions that had an equal transmission distance between the track and transducer. An averaged spectrum for a particular passing speed and receiver distance was then calculated by averaging over several equidistant accelerometer positions. Further, the ambient vibration level at the site was calculated from conducted background measurements, averaging over a total of 7 measurement positions. For the background vibration level, a Hanning window function and amplitude scaling factor of 2 was applied due to the signal type, a random noise time signal with rather constant vibration amplitudes. The Signal-To-Noise Ratio (SNR) was determined to be at least 17 dB, generally higher, for all bands of all averaged passage spectra. The determined ratio was considered sufficient, and no correction for background noise was performed to any of the computed spectra.

As mentioned earlier, the complete Matlab script used for data processing is presented in Appendix C.

5

Comparison Study - Predictions versus Measurements

This chapter describes the method used for the comparison of HS2 predicted vibration spectra of the Regina train, with the computed measurement spectra from Greby, Skövde. It describes the assumptions made in order to enable calculations, due to the limited input data. An explanation of how the HS2 model script was set up and used in order to generate predictions is given.

To enable calculations using the implemented Matlab model, some assumptions and approximations were needed. A very limited amount of data on unsprung masses of different trains were found. Even in the HS2 documents, no information on average unsprung mass of the reference trains Eurostar 373 or CL322 are presented. Therefore, the assumption that the reference train and proposed train have equal unsprung mass was made, which then needs to be considered a factor of uncertainty when interpreting the results. In the script after the unsprung mass correction, one has to input the train-track dimensions of both the reference train and proposed train into the loop that calculates the effective roughness of both trains. None of the dimensions mentioned in Figure 2.10, relevant to the Eurostar 373 or CL322, are mentioned in the HS2 document. However, the total length of a Eurostar 373 middle carriage (the most frequent carriage type in common Eurostar train sets) is stated to be 18700 millimetres according to [42]. Approximations of the different dimensions had to be conducted for all trains used in the comparison, namely Eurostar 373, CL322 and Regina. Together with side-view pictures of the trains, the other dimensions were approximated by measuring in the photos (mm per pixel using a pixel ruler tool). The wheel base of Regina trains is declared to be 2700 millimetres according to [24], and the total length of CL322 carriages is stated to be 19950 millimetres according to [43]. The sleeper spacing of the BR and SNCF ballast tracks are 650 and 550 millimetres respectively [5]. For the Regina train it was assumed that the sleeper spacing is equal to the standard spacing for all new railway constructions in Sweden, which is 600 millimetres according to [25]. The dimensions used for the comparison study are summarized in Table 5.1 below. The generic roughness spectrum used in the HS2 model only has data of wavelengths up to 25 metres. Since dimension e for the Regina train is circa 29 metres, it was set to 25 metres in the model. The approximations of the train dimensions have to be considered a possible source of error when comparing predicted versus measured spectra.

Table 5.1: Track-train dimensions used for calculation of HS2 vibration spectra, equivalent to measurement spectra. The dimensions are presented in millimetres.

	a	***b***	***c***	***d***	***e***
Train type:	-	-	-	-	-
Eurostar 373	550	3320	3320	15405	21978
CL322	650	2800	4912	9928	22677
Regina	600	2700	4800	16080	28980

After specifying the dimensions for the reference train and proposed train, the A and B constants for the parabolic functions describing the parametric excitation were set to 5 dB and 0.05 metres respectively (these can however be used to tune the model). Once the effective roughness spectra for the two trains were computed, they were related to their respective train speed, reference train speed and proposed train speed. From the one third octave band difference between the effective roughnesses, the speed and track-train correction was calculated and used to correct the proposed train vibration spectrum with. After this correction, one of the three insertion losses defined in the model is assumed for the proposed train (SNCF ballast, BR ballast or BCT) and corrected for as described earlier. Lastly, depending on lithology, the two spectra are adjusted in order to account for the transmission between source and receiver. For comparisons, the receiver distance R was set to calculate equivalent transmission in the model as for the measurements, which was between rail centre-line to accelerometer position. The measurement receiver distances were measured from the rail centre-line and the HS2 model calculates from the nearest rail of the track, meaning a difference in half of the track gauge has to be accounted for, which is 717.5 mm for Swedish standard track gauge. With the assumptions described in this paragraph, predicitons of Regina passages using the implemented model could be performed.

For the comparison study, measurement spectra equivalent to the predictions had to be calculated. This was done by summarizing and computing averaged one third octave band spectra for passages of the Regina train at 250 km/h, 200 km/h and 150 km/h, at two different receiver distances, 10 metres and 25 metres. This was done as described in Section 4.2, and generated six separate averaged vibration level spectra to be used for comparison with their equivalent model prediction. Figure 5.1 presents an example of one measurement passage. The levels of the separate equidistant measurement points and their average are plotted, as well as the average background level.

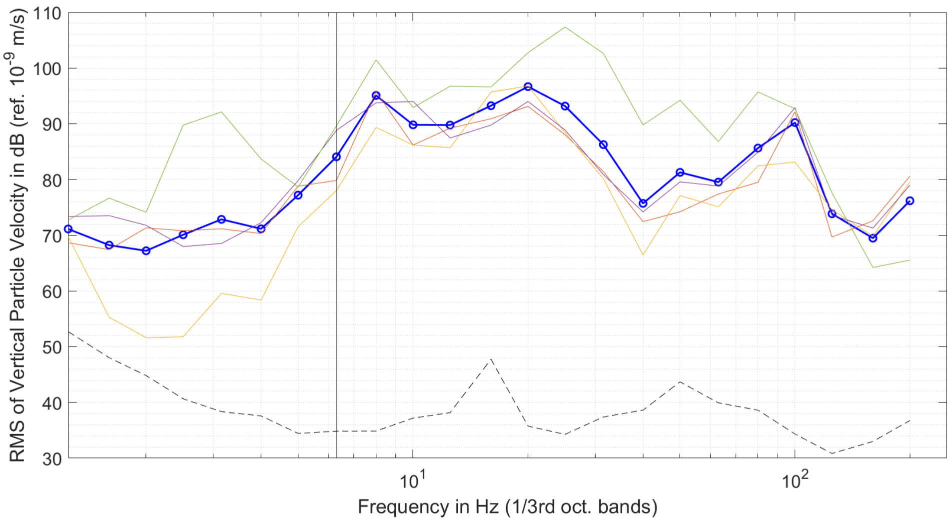

Figure 5.1: Measurement data from passage of the Regina train at 25 metres from the centre-line between the rails of the western track. Train speed: 250 km/h. The thin solid lines are the levels at the separate accelerometer positions (positions 5, 9 and 13, accelerometer mounted on a metal ground spike secured in the surface ground layer). The solid circle-marked line presents the calculated average between the measurement points. The thin dashed line is the averaged background vibration level. The vertical line is located at 6.3 Hz, the lower end of the HS2 model frequency range.

The ground material of the measurement location, glacial clay, is not explicitly defined in the HS2 model. Therefore, the step after summarizing the measurement averages was to identify which of the generic lithology that produce spectra with the highest correlation to the glacial clay measurement spectra. Furthermore, the assumed track system of the proposed train affects the predictions computed by the model. Therefore, there was a need to determine the track system and lithology combination that provided the most accurate predictions for Regina on Swedish standard ballast track and glacial clay. An effort to compute the HS2 spectra using all of the different lithologies in combination with the different track systems was performed, which in the end generated twelve HS2 predicted spectra to compare with each measurement spectrum (4x ground material types with their respective reference spectrum and 3x track systems with their respective insertion loss). An example plot of one of these comparisons is presented in Figure 5.2.

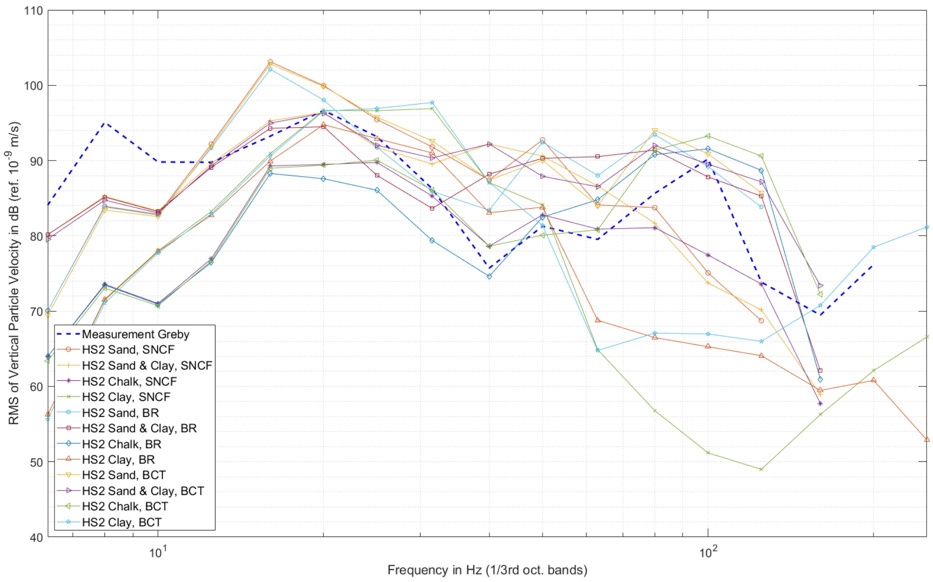

Figure 5.2: Example plot of the comparison between HS2 predictions with different lithologies and different track systems, versus averaged measurement data. Regina train passage at 250 km/h on glacial clay, receiver position at 25 metre distance.

Six separate plots as the one presented in Figure 5.2 were used to determine the appropriate ground material and track system combination for modelling glacial clay and the Swedish track system, at the site in Greby. In order to quantify the similarity between a prediction and measurement curve, the absolute value of the difference in each one third octave band was calculated, and then summed. The HS2 ground material and track type combination with the lowest value exhibits the most similar trends with the measurement spectrum curve. This combination was declared the most suitable to use for predictions of the considered case, glacial clay at this specific site. Further analysis using only the identified ground material and insertion loss combination was then performed, in order to investigate the differences in spectral components and to deduce potential limitations of the model and its predictions, etcetera. The continued analysis also included tuning of the model's A and B parameters for the parabolic functions, to provide a better fit to measured data. The results from the comparison study are presented in Chapter 6.

6
Results and Discussion

This section presents the results generated within the thesis project as a whole. This includes results and discussion on the implemented HS2 model predictions and the comparison investigation. The model itself is analysed and discussed. Further, factors of uncertainty, plausible limitations of the model and potential adaptations are presented. Proposals for continued work are stated at the end of this chapter.

6.1 Results and Discussion of the Implemented HS2 Model Predictions, Measurement Data Processing and Comparison Study

The processing of measurement data resulted in six averaged spectra of the Regina passages. As stated previously, the averages were derived from multiple measurement points per train speed, and were calculated using the previously presented processing technique. Not all measurement point time signals were possible to use for the data processing (due to e.g. sensor overloading and/or generally faulty time signals with obscure trends and levels). This means that the average of each measurement spectrum has been taken of a varying number of sensor signals, and the accuracy could possibly be improved for future measurements. Also, analysis of the separate measurement points revealed that there can be a relatively large spread in vibration level between points, particularly at 25 metre receiver distance and for frequencies from around 4-7 Hz and below (see the low frequency range of Figure 5.1). This could be due to low frequency resonances in the ground layer profile and/or other propagation effects, producing a complex wave pattern where the soil response at the surface differ significantly from positions to position. This could mean difficulty of estimating vibration at low frequencies, and might be a reason for why the HS2 model is only valid for frequencies down to 6.3 Hz. Moreover, when analysing the averaged measurement curves, it is difficult to deduce if there are any frequency components/spectrum peaks that relates to a potential resonance in the accelerometer mountings, which has been discussed previously, and can be a possible source of deviance between prediction and measurement. Conducting new train passage measurements under Swedish conditions for several more ground material types, with the aim of using in continued work of this thesis would be advantageous. However, planning measurements of train passages require a substantial amount of preparation and resources, and due to the limited time-frame of the thesis, the acquired measurement data was the only feasible option for comparing predictions with real measurement data.

From the six comparisons of the Regina measurements with HS2 predictions of all defined ground material types within the model, and in combination with one of the three different track systems (according to the evaluation procedure presented in 5.). Out of the six comparisons, sand & clay mixture on BR ballast produced values closest to the measurement curve two out of six times, sand & clay mixture on SNCF ballast one out of six times and sand on SNCF ballast three out of times. The results are slightly ambiguous, however, they indicate that sand & clay mixture with British track and/or sand with French produce the highest correlation to measured data. This seems reasonable due the the description of glacial clay as presented in Section 4.1. Glacial clay is a soil material with fine-grained cohesive clay mixed sporadically with sand and stone. Based on this finding, the two material/track combinations chosen for further analysis were sand & clay mixture on BR ballast track and sand on SNCF ballast track. The two combinations gave overall the best results for the particular location (glacial clay, 3-5 metre depth to bedrock, Swedish standard ballast rail system). Further, the ground material at the site has a load-bearing capacity and stiffness of that can vary drastically, and is dependant on e.g. water saturation, which in turn can differ over time due to seasonal changes etcetera. Moreover, the rather shallow depth to bedrock could possibly cause resonances in the ground layer profile. Due to the potential sources of error along the calculation chain, the results of the model are viewed as indicative, and predictions should still be performed with caution, and favourably verified by measurements. To be certain on the geological conditions at the measurement site, a seismic study would have to be conducted. It is possible that the measurement site ground material consist of glacial clay with high amounts of sand. Figure 6.1 presents all Regina measurements compared to the equivalent HS2 predictions of sand & clay mixture on BR ballast and sand on SNCF ballast. The blue solid lines with square markers represent the measurement spectra at the particular speed and receiver distance, the red solid line with circles represents the HS2 prediction of sand & clay mixture on BR ballast and the green solid line with crosses represents the HS2 prediction of sand on SNCF ballast. The blue dashed line is the single value of the measurement spectrum, the red dashed dotted line is the single value of the HS2 prediction of sand & clay mixture on BR ballast and the green dotted line is the single value of sand on SNCF ballast.

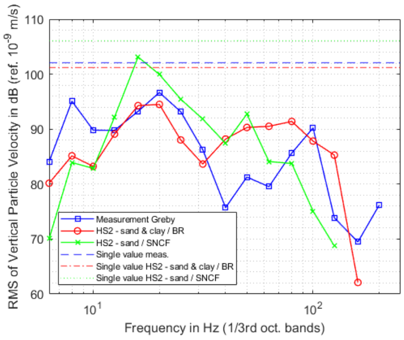

(a) 250 km/h, $R = 25$ m.

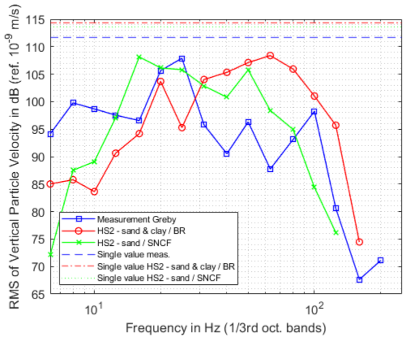

(b) 250 km/h, $R = 10$ m.

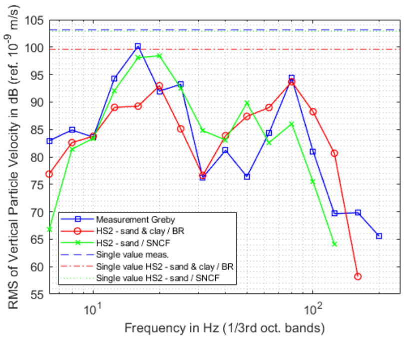

(c) 200 km/h, $R = 25$ m.

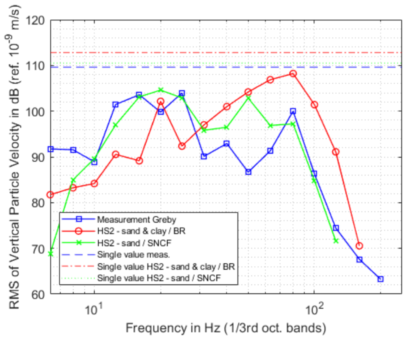

(d) 200 km/h, $R = 10$ m.

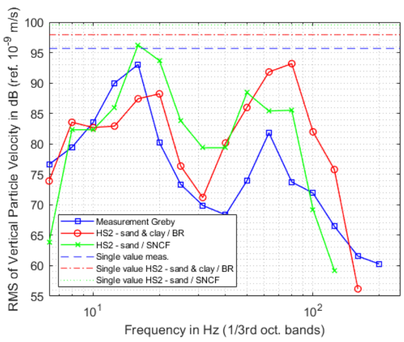

(e) 150 km/h, $R = 25$ m.

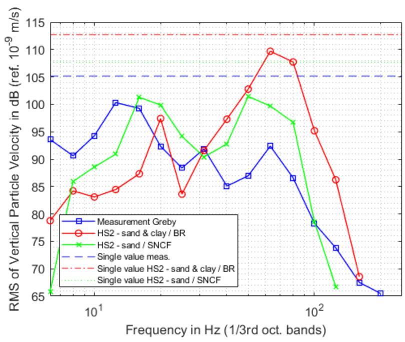

(f) 150 km/h, $R = 10$ m.

Figure 6.1: Comparison of Regina measurements at different speeds and receiver distances, versus HS2 predictions of Regina train as proposed train on sand & clay mixture / BR Ballast, as well as on sand / SNCF ballast.

When analysing the plots of Figure 6.1, it is realised that the general trends in the predicted spectra are to a certain extent similar to the measurement spectra. Separate band levels can vary significantly, but the overall magnitudes of the spectra seem to be at a reasonable agreement. The single values of four out of six comparison plots show that the HS2 model's single values are usually slightly higher than the measurement's. The average difference between the single values of measurement spectra versus sand & clay mixture / BR, and sand / SNCF have been calculated. They were calculated to be 1.9 dB and 2.2 dB respectively. Both values are rather close the measurement single value, which points towards a reasonable prediction accuracy when considering the total single value of the complete spectra, and not the exact frequency components of each band. Deviations between the spectra's separate bands are expected due to the possible error sources and assumptions that were needed to enable predictions in the first place. Factors of uncertainty are further discussed in the next section. In the frequency range from around 10 to 15 Hz and downwards (slight variations between separate plots in Figure 6.1), the HS2 model seems to predict lower levels when compared to the measurement curves, an under-estimation in this range (except for subfigure *e* in Figure 6.1). This holds for both material and track combinations used in the final comparisons. When looking at the HS2 reference spectra, is is realised that the general trend in the low frequencies is a roll-off in level. For most measurement spectra, there seem to be relatively high levels in the very low range, which is contradictory. This could mean differences in material properties and vibration response between central European soils (as the generic ones defined within the model), and Swedish soils. It would be of interest to extend the range of the HS2 model down in frequency (to reflect the ISO 14837 standard [2] range for low frequency vibration, 1 to 80 Hz), and evaluate the precision in this range. However, an extension would probably mean multiple more measurements to produce new source term spectra with sufficient statistical confidence. Also, as declared in the measurement data analysis section, there can be significant differences between separate measurement points at very low frequencies.

In Figure 6.1, there seems to be a systematic over-estimation in the mid/high frequency range, which is seemingly consistent through different comparisons. The exact range of the over-estimation of course varies for the separate plots. The plot of Regina at 200 km/h, 25 metre receiver distance is the only comparison where the the measurement's single value is higher than the both of the predicted single values. When analysing the overall shape of the predictions curves, they seem to decently follow changes in receiver positions, and different speeds. This indicates that the model can be used successfully for the analysed case, under Swedish conditions. This model is used for noise and vibration assessments (environmental assessment model as declared in the standard ISO 14837 [2]), and is seemingly not derived for detailed analysis. Therefore, it would probably be sufficiently accurate to use for Swedish conditions at an environmental assessment level, but validation measurements are still recommended. It could be advantageous to derive new source term spectra and propagation terms specific to generic Swedish ground materials and common Swedish trains.

As a test, the model's A and B parameters for the parabolic functions were adjusted for one of the comparisons plots to see if the predictions could be tuned to provide a better fit to measured data. The 200 km/h and receiver distance 25 metres was chosen for this study. For all comparisons in Figure 6.1, A and B were set to 5 dB and 0.05 metres respectively. In an iterative way, both the parameters were altered in small increments up and down. Ultimately, a set of parameter values that provided a slightly better fit between predictions and measurement was found. These where A = 8 dB and B = 0.06 metres for sand & clay mixture / BR, and A = 5 dB and B = 0.06 metres for sand / SNCF. Two plots from this study are presented in Figure 6.2 and Figure 6.3. The spectrum of the reference trains were also included in order to visualize the effect of the HS2 model corrections.

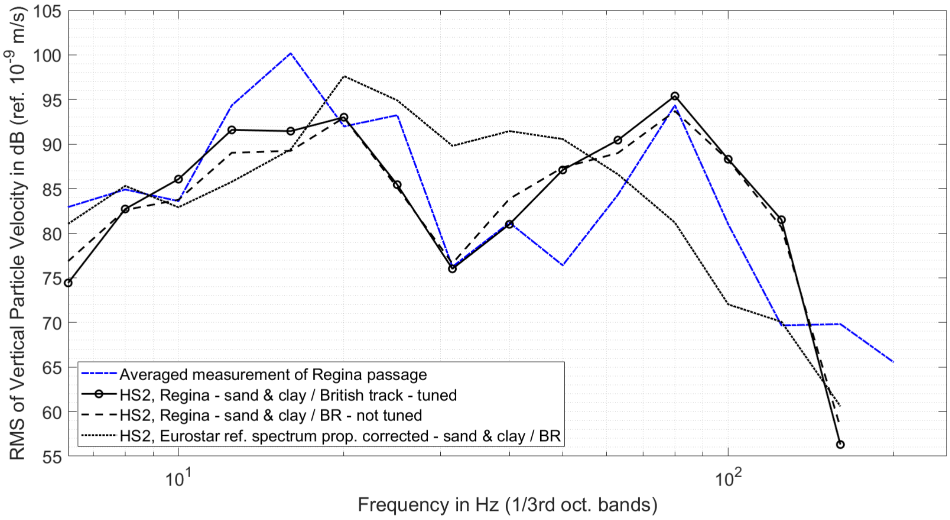

Figure 6.2: The resulting HS2 predictions of sand & clay / BR after tuning the coefficients of the parabolic functions for the proposed trains. Regina passage measurement at 200 km/h, receiver distance 25 metres.

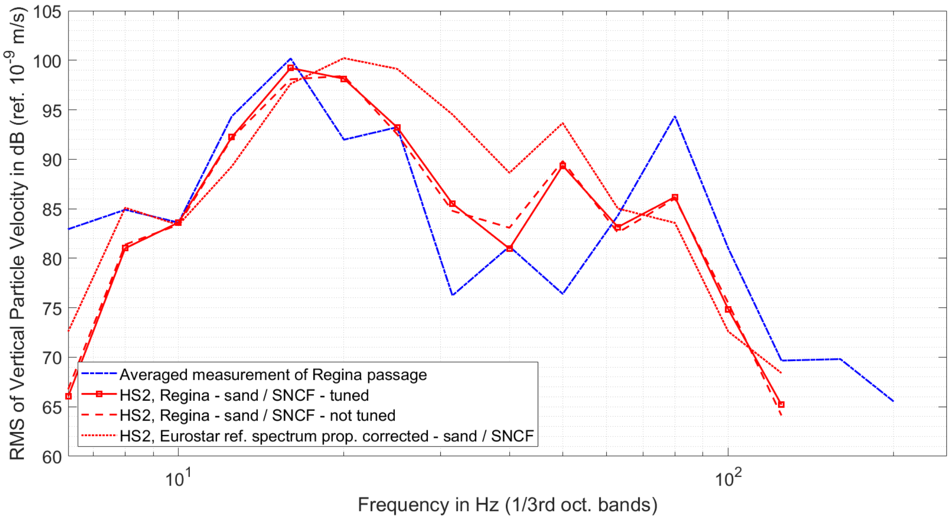

Figure 6.3: The resulting HS2 predictions of sand / SNCF after tuning the coefficients of the parabolic functions for the proposed trains. Regina passage measurement at 200 km/h, receiver distance 25 metres.

Both the tuned prediction curves in Figure 6.2 and Figure 6.3 follow the measurement curve quite well. One major difference for the tuned sand / SNCF curve is at 50 Hz, where the prediction presents a peak and the measurement a dip. The peak at 80 Hz can be seen in the sand / SNCF graph and the measurement curve, but it differs in magnitude. For the tuned sand & clay mixture / BR curve the peak at around 16 Hz is flat when compared to the measurement curve, and the peak around 80 Hz is for this material / track combination wider than sand / SNCF. Both material / track combinations present an under-estimation in low frequencies, with the most deviance to the measurement curve occurring for sand / SNCF. Further, when studying the curves which represent the reference trains (reference spectra only corrected for propagation), it can be seen that the model's corrections are producing proposed train curves that fit much better to measurement data. The used reference spectra are Eurostar 373 at 250 km/h for sand & clay mixture, and 268 km/h for sand, with propagating corrections for 25 metre receiver distance and the respective material coefficients.

6.2 Analysis and Discussion of the HS2 Prediction Model

This section presents an analysis and discussion on the HS2 prediction model, with its limitations in focus. Further, possible error sources within the model is also discussed.

The HS2 model utilizes empirically acquired data for the reference spectra defined in the model. There is no information in the model description documents on how the reference spectra of the generic ground materials were derived, for example if some sort of average is utilized or not. Obviously, the inherent shape and magnitude of the used reference spectrum affects the spectrum shape of the proposed train, with artifacts that can be seen when comparing the reference spectrum with the proposed spectrum. This is unavoidable when utilizing reference data to compute predictions. All of the model's reference spectra are measurements of the vibration level at 10 metres from the nearest rail of the track, and it would be possible to derive several more spectra for other materials. For further work, it would be advantageous to compare further measurements with model predictions for even more types of ground materials. However, as seen in the comparison study, the model does pretty well when predicting the single value of a train passage, usually with slight over-estimation of levels. The model can be tuned to achieve even better accuracy. Nevertheless, empirical and numerical models are only approximations of the real life case, and there will always be deviations depending on quality of input data, setup of model parameters, measurement artifacts etcetera. To minimize the influence of crude assumptions and other possible error sources, it is important to identify and document the factors of uncertainty and how they affect the results. The following section incorporates a list which summarize the possible limitations and factors of uncertainty within the HS2 model.

6.2.1 HS2 Model Limitations and Factors of Uncertainty

a. As stated in [5] and [6], a limitation of the model could be the fact that it only models the vertical vibration component. Vibration is a three dimensional phenomenon, and all three axes influence the particle motion in the medium, and thus the resulting vibration at a receiver position. According to the model documents, low to mid-rise building are generally more susceptible to vibration in vertical direction, and human receivers are more sensitive to vibration in vertical direction, i.e. from feet to head. The model does not seem to take into account if a person is in recumbent position e.g. during sleep (and the model is still used for calculating comfort during night time). This orientation would mean that humans have a different sensitivity to vibration, which complicates the problem further.

b. A limitation in the model is due to the available data for the generic roughness function that is utilized in order to model the excitation of wheel and rail roughness. This function also influence the parametric excitation (the parabolic functions are superimposed onto the generic roughness curve). The measured roughness spectrum only contains roughness amplitude values to model wavelengths down to 25 metres. This means that the model can not handle wavelengths above 25 metres. For example, during this thesis is was found out that one of the dimensions of Figure 2.10 (derived in ISO 14837 [2]), of the Regina train is above 25 metres, meaning that this parabolic function could not be superimposed onto the roughness curve, hence no contribution from this dimension. As stated before, in the study of the Regina train, this dimension was set to exactly 25 metres (the actual dimension is approximately 29 metres), which is a possible factor of uncertainty of the computed HS2 spectra. However, one Regina HS2 spectrum was checked with and without this parabolic term, and the difference was considered minor.

c. The A and B constants for the parametric excitation have to be set to a particular level and wavelength respectively. These assumptions directly influence the levels and overall shape of the predicted vibration spectrum. These constants can be tuned to provide a better fit between predictions and measurements. An effort to tune the parameters were conducted with favorable results as described previously. In that study, A and B were set to the same value for all calculated parametric terms, for each material/track combination. However, the constants could possibly be set to individual values per track-train dimension (five separate L_K parabolic functions with separate A_K and B_K values). This might provide better accuracy, but yields difficulties when conducting predictions without measurement data for validation of the predictions.

d. Another possible error source in the calculations can arise from inaccurate input data, for example inaccuracies the dimensions for the parametric excitation. As stated previously, it proved difficult to acquire all the data needed to model the trains. Limited technical specifications of the trains were found. Instead, approximations had to be utilized. This, in turn, affect the train specific effective roughness. Nevertheless, a fairly good correlation was achieved in the comparison between measurements and predictions, which indicates that the assumptions are probably reasonable.

e. The HS2 model's frequency range spans from 6.3 to 250 Hz. According to ISO 14837 [2], the relevant frequency range for ground-borne noise and vibration spans from 1 to 250 Hz, with low frequency vibration occurring between 1 to 80 Hz. This is a limitation of the model. Building and floor span resonances are usually found at very low frequencies. It might be appropriate to extend the frequency range to around 1 Hz in order to draw more accurate conclusions for very soft ground materials and for assessing the risk of coinciding with building eigenfrequencies. However, ISO 14837 [2] states that in general, the critical frequency range for response of building elements is between, 1 to 100 Hz, and most of this range is covered within the model calculations.

f. The HS2 model uses a generic roughness profile derived from several measurements as described in Section 3.2. Obviously, the roughness depend on tolerances, manufacturing, corrosion as well as wear and tear over time. The roughness will therefore be slightly different between a new and an older well used track. Also, the roughness profile of Swedish ballast track system might differ from the HS2 model's.

g. The conducted analysis of this study has shown that the assumed insertion loss has a relatively large influence on the predicted vibration levels. This certainly applies to the higher end of the frequency range, where the difference between the models included insertion losses can be rather drastic, from around 70 Hz and upwards. A calculation of the insertion loss of the track on which the proposed train is running on would probably increase the accuracy of the predictions (for example the insertion loss for Swedish standard ballast track for the Regina case).

h. Obviously, the ground material plays a large role in the transmission of vibration to the surroundings. The possible influences have been discussed previously. Ground material type, water saturation, inhomogeneities, complex wave patterns due to ground layer resonances, wave-guiding due to topology and more, are all examples of possible factors influencing the vibration spectrum at a receiver position R metres form the track. Since the behaviour of the ground layer profile can vary drastically from case to case, it is possible that the model sometimes produce a propagation correction that differs from the real life case.

i. A limitation of the model is also that two out of the four defined reference spectra are missing level data in the upper frequency range. This can be seen in Figure A.1 in Appendix A. The two lithologies with limited data are sand and sand & clay mixture.

6.2.2 Proposals for Continued Work

The topic of train related ground vibration is comprised of several subjects within science and engineering. To allow for such a multidisciplinary study to be conducted within the given time-frame of this thesis, relevant limitations had to be set. This means that interesting subjects are explicitly stated to be out of scope, which could be studied if further time is given. The following section aims to document some of the topics of potential continued work.

The first idea for continued work is to utilize the developed Matlab model in further comparisons with measured data. Therefore, several measurements of train passages of e.g. the Swedish high-speed train X2000 and freight trains on different ground materials would need to be conducted. Preferably with some geological/seismic investigation to accompany the measurement data. By conducting measurements with the aim of using them to compare with the developed HS2 model script's predictions, the measurements can be setup to achieve accurate data for the particular task at hand. It would be recommended to measure with accurate seismic accelerometers (with a frequency response down to around 1 Hz). A proposal for measurement positions could be; on the rail, 10 metres, 25 metres and 40 metres. During the measurements, it is recommended to keep an accurate record of the passing trains, and to record the speed of each train. Recording the speed could preferably be done with a lidar gun, but also by means of video recording perpendicular to the railway track. A video recording would also make it possible to identify the setup of the train-set, as well as approximate axle distances and so on. Regarding the ground layer materials, it would be of interest to measure on two locations where the lithology is as close to the HS2 defined generic lithologies as possible, for example identify and measure on sand & clay mixture or pure clay as the main material body supporting the railway track system. It would also worthwhile to measure an extreme case, were the ground material is very loose (for example on muck or ooze), and compare to HS2 predictions. It is recommended to measure at sites were the depth to bedrock is as large as possible, in order to avoid ground profile resonances. If several measurements are to be conducted, new vibration source terms and for other ground material types and Swedish trains might be possible to derive, which could make the model more accurate for Swedish conditions. Propagation coefficients for the added ground material types would also have to be calculated.

Further, continued work of adapting the model to Swedish conditions could be performed with regards to the roughness profile used in the calculations, and the insertion loss spectrum. Also, if the effective roughness profile could be measured for longer wavelengths, the model might be applicable for lower frequencies than 6.3 Hz. Regarding the roughness profile, a function derived from measurements on Swedish standard rail system and rolling stock would have to be conducted. If this roughness profile differs drastically from the generic profile used in the HS2 model, the Swedish one could be utilized for the calculations instead. However, for this derivation, more in-depth information on how the insertion losses of the model were derived, information on the used reference and so on. A measurement with equivalent prerequisites would then have to be setup and conducted.

An effort to compile a database with technical information on the reference trains of the HS2 model and Swedish trains could be performed, in particular of the high-speed trains under operation in Sweden. This database would preferably include the train dimensions discussed earlier, the standard sleeper spacings, average unsprung masses, total weights and also information on common train-set configurations. Lastly, the current implemented HS2 Matlab script could be expanded in order to allow for calculations on Green's tunnel sections, as well as for tunnels. Further, the last steps of the model that include weighting and event $eVDV$ could be programmed. These steps can also be adapted in order to compute weighting etcetera, using Swedish standard metrics.

7 Conclusion

This thesis can be characterized as distillation of several broad and complex subjects, down to the relevant information for the particular task. Focus was kept on the initial aim, objectives and demarcations. Firstly, based upon the conducted investigation, it is possible to utilize the default HS2 prediction model to compute relatively accurate predictions for Swedish conditions, with the model's included reference data. It was possible to model the particular studied case, i.e. glacial clay, fairly well. It was determined that using the model with the material / track combinations of sand & clay mixture / BR ballast track or sand / SNCF ballast track, produced the highest correlation between predictions and measurements. Due to the description of glacial clay, it is expected that one of these ground material types would produce the best results. The calculated single values of measurement versus predictions are within -3.6 to +7.7 dB for all final comparisons (Figure 6.1). When looking at the complete spectrum, the model seems over-estimate vibration levels for the majority of the separate comparisons. The difference per one third octave band can vary, and there are occasions where the model can not approximate some of the peaks of the measurement data spectra. However, the model captures the major peaks, and the overall magnitude is reasonably accurate when compared to measurement data. An over-estimation of vibration level can lead to expenses by means of major noise and vibration mitigation measures, but one could argue that this is more advantageous than an under-estimation. An under-estimation could ultimately lead to noise and vibration issues not being identified. The model is seemingly aimed for noise and vibration assessment on a "macro-level" in an intermediate project phase, i.e. not for detailed study of for example the exact frequency content of one passage event. With regards to low frequencies, the model seemingly under-estimates vibration levels in the lowest part of the frequency range, when comparing with measurement spectra. This is important to consider when utilizing the model for calculations on soft ground materials. Also, as discussed earlier, it might be of value to extend the model by means of including reference data for more ground materials and track systems, and by incorporating reference data for lower one third octave bands than the current lowest of 6.3 Hz. This could possibly enhance the accuracy of the predictions, especially for low frequencies were all measurements studied in the Swedish case present relatively high levels in the lowest part of the frequency range. However, several more measurements of train passages under Swedish conditions are needed for continued work of adapting the model.

One of the main deliveries of this thesis is the developed Matlab script of the HS2 model, based on the model documents and papers. So with reference to the questions stated in the beginning of the report, it is possible to program the HS2 model in Matlab in a useful way for vibration level estimation. The model is relatively straight forward to setup and use for noise and vibration predictions. It is considered a rather quick and easy methodology for vibration estimation, if correct input data is available and/or if adequate assumptions are made. Also, the script for measurement data processing can be useful for future work.

Bibliography

[1] D. Gubler, *"File:Eurostar Class 374 on HS1.jpg," Wikimedia Commons*, [Online], Sept. 2015. Available: https://commons.wikimedia.org/wiki/File:Eurostar_Class_374_on_HS1.jpg

[2] *Mechanical vibration - Ground-borne noise and vibration arising from rail systems*, ISO 14837, 2005.

[3] "High Speed 1," *HS1 Ltd*, 2021. [Online] Available: https://highspeed1.co.uk/

[4] "High Speed 2," *High Speed Two Ltd 2021*, 2021. [Online] Available: https://www.hs2.org.uk/

[5] "London - West Midlands Environmental Statement," High Speed Two Limited, England, Volume 5 Appendix SV-001-000 ES 3.5.0.10, Nov. 2013. [Online] Available: https://webarchive.nationalarchives.gov.uk/20140613014254/http://assets.dft.gov.uk/hs2-environmental-statement/volume-5/sound/Vol5_Appendix_SV-001-000.pdf

[6] "High Speed Rail (West Midlands - Crewe) Environmental Statement," High Speed Two Limited, England, Volume 5 Appendix SV-001-000 ES 3.5.0.15, Jul. 2017. [Online] Available: https://assets.publishing.service.gov.uk/government/uploads/system/uploads/attachment_data/file/628750/E61_SV-001-000_WEB.pdf

[7] V. Jurdic, O. Bewes, R. Greer and T. Marshall, "Developing Prediction Model for Ground-Borne Noise and Vibration from High Speed Trains Running at Speeds in Excess of 300km/h," in *The 21st International Congress on Sound and Vibration*, Beijing, China, 13-17 Jul. 2014. [Online] Available: https://www.semanticscholar.org/paper/developing-prediction-model-for-ground-borne-noise-jurdic-bewes/e4cf9c93ea171a60fb5c6a018f33042097d7c292

[8] T. Marshall, G. Sica, N. Fagan, D. Perez, O. Bewes and R. Thornely-Taylor, "The predicted vibration and ground-borne noise performance of modern high speed railway tracks," in *Internoise 2015*, San Fransisco, CA, USA, 9-12 Aug. 2015. [Online] Available: https://www.researchgate.net/

publication/308308486_The_predicted_vibration_and_ground-borne_noise_performance_of_modern_high_speed_railway_tracks

[9] T. Ekevid, "On Computational Wave Propagation in Solids - with Emphasis on High-Speed Train Related Ground Vibrations," Licentiate Thesis, Dept. Struct. Mech., Chalmers Univ. of Tech., Gothenburg, Sweden, 2000.

[10] B. A. Bolt, *Earthquakes: Newly Revised and Expanded.* New York, NY, USA: W. H. Freeman and Company, 1993.

[11] A. V. Shoushtari, "Seismic Hazard Assessment of Peninsular Malaysia Based on New Ground-Motion Prediction Equations for Subduction Earthquakes," Ph.D. dissertation, Fac. Civ. Eng., Univ. Tech. Malaysia, Johor, Malaysia, 2016. [Online] Available: https://www.researchgate.net/publication/327894248_SEISMIC_HAZARD_ASSESSMENT_OF_PENINSULAR_MALAYSIA_BASED_ON_NEW_GROUND-MOTION_PREDICTION_EQUATIONS_FOR_SUBDUCTION_EARTHQUAKES.

[12] L. Rayleigh, “On Waves Propagated along the Plane Surface of an Elastic Solid,” Proc. Lond. Math. Soc. 14, 4, 1885. [Online] Available: https://londmathsoc.onlinelibrary.wiley.com/doi/abs/10.1112/plms/s1-17.1.4

[13] L. Bergmann and H. Hatfield, *"Ultrasonics and their scientific and technical applications,"* New York: J. Wiley and sons, inc., 1942.

[14] "SGF Infromationsskrift 1:2012 Markvibrationer Version 2013-12-18" (text in Swedish), *Swedish Geotechnical Society*, Dec. 2013. [Online] Available: http://www.sgf.net/getfile.ashx?cid=495387&cc=3&refid=5

[15] H. Lamb, "On the Propagation of Tremors over the Surface of an Elastic Solid," Royal Society of London, 1904. [Online] Available: https://royalsocietypublishing.org/doi/10.1098/rsta.1904.0013

[16] T. Waltham, *Foundations of Engineering Geology*, 3rd ed., London, England: Spon Press, 2009.

[17] G. Sällfors, *Geoteknik* (book in Swedish), 3rd ed., Gothenburg, Sweden: Vasastadens Bokbinderi AB, 2003.

[18] “Jordmateriallära” (text in Swedish), *Swedish Geotechnical Institute,* Dec. 2020. [Online] Available: https://www.sgi.se/sv/kunskapscentrum/om-geoteknik-och-miljogeoteknik/geoteknik-och-markmiljo/jordmateriallara/

[19] J.M. Head and F.M. Jardine, "Ground-Borne Vibrations Arising from Piling," CIRIA, London, England, Rep. 142, 1992.

[20] "Geological Survey of Sweden," *Geological Survey of Sweden.* [Online] Available: https://www.sgu.se/en/

[21] "Geokartan," *Geological Survey of Sweden.* [Online] Available: https://apps.sgu.se/geokartan/#mappage

[22] B. Möller, R. Larsson, P. E. Bengtsson and L. Moritz, "Geodynamik i praktiken" (text in Swedish), *Swedish Geotechnical Institute,* Linköping, Sweden. 2000. [Online]. Available: https://www.sgi.se/globalassets/publikationer/info/pdf/sgi-i17.pdf

[23] *"File:LGV Interconnexion Est - Moussy-le-Neuf 01.jpg," Wikimedia Commons*, [Online], Apr. 2014. Available: https://commons.wikimedia.org/wiki/File:LGV_Interconnexion_Est_-_Moussy-le-Neuf_01.jpg

[24] *"Motorvagnståget Regina,"* Bombardier Transportation, Västerås, Sweden. [Online] Available: https://www.transitio.se/Documents/document/Produktblad%20Regina%204sid_LR.pdf

[25] TDOK 2013:0664 Banöverbyggnad - Skarvfritt spår, krav vid byggande och underhåll (documents in Swedish), Version 1.0.0, The Swedish Transport Administration, Borlänge, Sweden, Apr. 2020. [Online] Available: https://puben.trafikverket.se/dpub/visa-dokument/1b9a2602-6dca-4675-ae54-80a6bc53bbbe

[26] *"File:PW-220K bogie of WE25T 600101 (20181223141835).jpg," Wikimedia Commons*, [Online], Dec. 2018. Available: https://commons.wikimedia.org/wiki/File:PW-220K_bogie_of_WE25T_600101_(20181223141835).jpg

[27] *"File:Concrete sleepers on the Main Southern railway line.jpg," Wikimedia Commons*, [Online], Mar. 2011. Available: https://commons.wikimedia.org/wiki/File:Concrete_sleepers_on_the_Main_Southern_railway_line.jpg

[28] V.V. Krylov (editor), *Noise and Vibration from High-Speed Trains*, London, England: Thomas Telford Limited, 2001.

[29] "Railway Induced Vibration - State of the Art Report," International Union of Railways, Nov. 2017. [Online] Available: https://uic.org/IMG/pdf/uic-railway-induced-vibration-report-2017.pdf

[30] W. Björkqvist and I. Janjua, "Evaluation and Comparison of Ballastless Track Systems with Regards to System and Performance Characteristics," M.S. thesis, in Mech. Eng., KTH Royal. Inst. of Tech. Stockholm, Sweden, 2020. [Online] Available: http://kth.diva-portal.org/smash/get/diva2:

1464116/FULLTEXT01.pdf

[31] *Mechanical vibration and shock — Mechanical mounting of accelerometers*, ISO 5348, 2021.

[32] *Human response to vibration - Measuring instrumentation*, ISO 8041, 2005.

[33] *Vibration and shock – Evaluation of human exposure to whole-body vibration*, ISO 2631.

[34] P. Persson, "Vibrations in a Built Environment - Prediction and Reduction," PhD thesis in Struct. Mech, Lund Uni. Lund, Sweden, 2016. [Online] Available: https://lup.lub.lu.se/search/ws/files/7485166/Thesis_web1026.pdf

[35] "Ny Vibrationsmodel Teknisk Rapport," Cowi A/S, Lyngby, Denmark, Jan. 2015. [Online] Available: https://docplayer.net/57400267-Januar-2015-banedanmark-new-vibration-model-technical-report.html

[36] A.M. Kaynia and G. Saygili, "Predictive Models for Earthquake Response of Clay and Sensitive Clay Slopes," Norwegian Geotechnical Institute, Oslo, Norway and Dep. of Civ. Eng., Uni. of Texas at Tyler, Tyler, TX, USA, Jul. 2014. [Online] Available: https://ngi.brage.unit.no/ngi-xmlui/handle/11250/2375331

[37] "Crossrail Information Paper, D10 - Groundborne Noise and Vibration," Crossrail, London, England, Apr. 2008. [Online] Available: https://2577f60fe192df40d16a-ab656259048fb93837ecc0ecbcf0c557.ssl.cf3.rackcdn.com/assets/library/document/d/original/d10groundbornenoiseandvibration.pdf

[38] N. Triepaischajonsak, D. Thompson, C.J.C. Jones, J. Ryue and J.A. Priest, "Ground Vibration from Trains: Experimental Parameter Characterization and Validation of a Numerical Model," Proceedings of the Institution of Mechanical Engineers Part F Journal of Rail and Rapid Transit 225(2):140-153, Mar. 2011. [Online] Available: https://www.researchgate.net/publication/258177602_Ground_Vibration_from_Trains_Experimental_Parameter_Characterization_and_Validation_of_a_Numerical_Model

[39] "Glaciala finkorniga sediment" (text in Swedish), *Geological Survey of Sweden.* [Online] Available: https://www.sgu.se/om-geologi/jord/fran-istid-till-nutid/isen-smalter/glaciala-finkorniga-sediment/

[40] J. Nyberg, "Beskrivning till maringeologiska kartan - Bottenviken" (document in Swedish), Geological Survey of Sweden, Uppsala, Sweden, 2016. [Online] Available: https://www.sgu.se/globalassets/produkter/kartor/

k539-beskrivning.pdf

[41] "fft - Fast Fourier transform," *Mathworks.* [Online] Available: https://se.mathworks.com/help/matlab/ref/fft.html

[42] "British Rail Class 373," *Wikipedia.* [Online] Available: https://en.wikipedia.org/wiki/British_Rail_Class_373#cite_note-3

[43] "British Rail Class 322," *Wikipedia.* [Online] Available: https://en.wikipedia.org/wiki/British_Rail_Class_322

A

Appendix A

Reference Data of the HS2 Prediction Model

The following tables include all of the reference data of the HS2 ground vibration prediction model, on surface level. The data was acquired from [6] and [5], where also data for the cases of bored tunnel to surface and Green tunnel can be found.

Table A.1: Reference source terms of the HS2 model. Vertical component root-mean-square of the particle velocity, level in dB with reference value 10^{-6} mm/s (Table 2, Annex D1 in [6].)

				1/3rd Oct. Band (Hz)	**6.3**	**8**	**10**	**12**	**15**	**20**	**25**	**31.5**	**40**	**50**	**63**	**80**	**100**	**125**	**160**	**200**	**250**
Train Type:	**Lith-ology:**	**Ref. Speed (km/h):**	**Ref. Dist. (m):**	**Ref. Track:**	-	-	-	-	-	-											
Eurostar	Sand	268	10	SNCF Ballast	74.5	88.4	93.8	102.3	106.0	108.7	108.7	104.7	101.0	105.7	98.2	93.9	81.2	75.3	-	-	-
Eurostar	Sand & clay	250	10	SNCF Ballast	85.6	86.0	83.4	87.3	89.5	106.2	101.7	108.6	107.3	106.1	103.1	94.6	84.2	79.7	72.0	-	-
Eurostar	Chalk	285	10	SNCF Ballast	69.0	78.2	74.2	75.9	85.8	93.6	98.9	96.6	91.2	96.0	93.2	92.3	87.0	87.7	77.6	66.7	59.2
CL322	Clay	100	10	BR Ballast	54.8	68.3	76.1	76.6	76.5	82.5	86.1	90.2	92.2	91.1	80.2	73.3	67.1	61.5	62.3	54.7	46.9

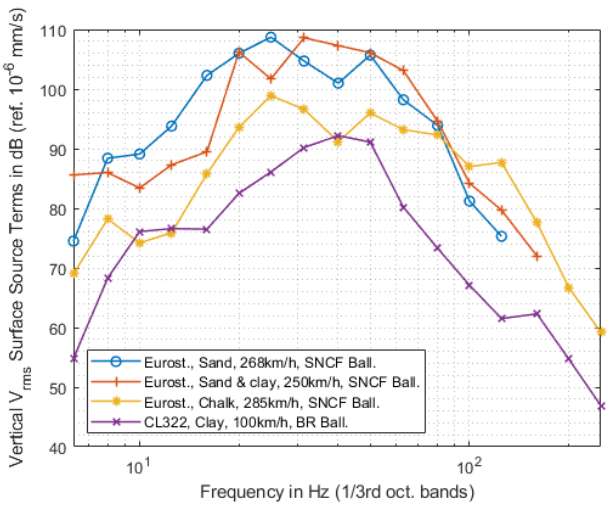

Figure A.1: The HS2 source terms of Table A.1 plotted over frequency.

Table A.2: Insertion losses in dB for the included track systems of the HS2 model (Table 3, Annex D1 in [6].)

	1/3rd Oct. Band (Hz)	**6.3**	**8**	**10**	**12**	**15**	**20**	**25**	**31.5**	**40**	**50**	**63**	**80**	**100**	**125**	**160**	**200**	**250**
Track Type:	**Sleeper spac. (m):**	-	-	-	-	-	-	-	-	-								
SNCF Ballast	0.55	0.0	0.0	-0.1	-0.2	-0.5	-1.1	-2.3	-4.1	-6.0	-7.5	-8.6	-10.3	-9.5	-5.5	2.1	5.1	17.5
BR Ballast	0.65	0.0	-0.1	-0.2	-0.7	-1.5	-3.0	-6.0	-10.0	-10.0	-7.8	-4.7	-0.6	4.6	9.6	5.3	3.8	3.8
Base Case Track	0.60	-0.6	-0.5	-0.4	-0.5	-0.8	-1.2	-2.0	-3.3	-6.0	-10.2	-8.7	0.0	6.3	11.5	16.6	21.5	32.1

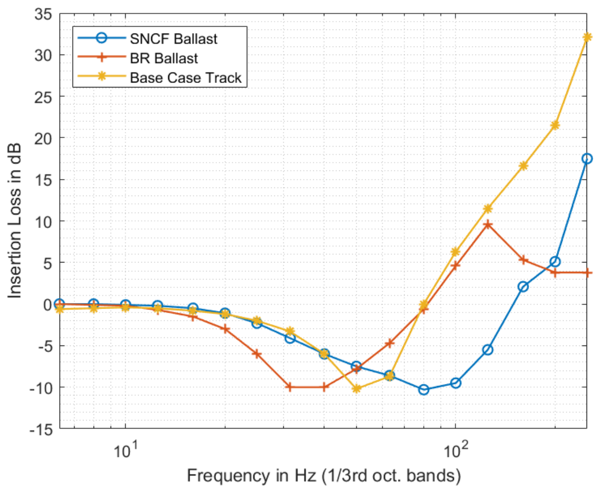

Figure A.2: The HS2 insertion losses of Table A.2 plotted over frequency.

Table A.3: Effective roughness function of the HS2 model (Table 4, Annex D1 in [5]). A total of 35 separate wavelengths with corresponding level in dB, reference value 10^{-9} metres.

Wave-length (m):	**25.0000**	**20.0000**	**16.0000**	**12.5000**	**10.0000**	**8.0000**	**6.3000**	**5.0000**	**4.0000**	**3.1500**
Level (dB):	55.0	54.0	53.0	52.0	51.0	48.1	45.0	42.0	39.1	35.9
2.5000	**2.0000**	**1.6000**	**1.2500**	**1.0000**	**0.8000**	**0.6300**	**0.5000**	**0.4000**	**0.3150**	**0.2500**
32.9	30.0	27.1	23.9	21.0	19.5	18.0	16.5	15.0	13.5	12.0
0.2000	**0.1600**	**0.1250**	**0.1000**	**0.0800**	**0.0630**	**0.0500**	**0.0400**	**0.0315**	**0.0250**	**0.0200**
10.5	9.1	7.5	6.0	4.5	3.0	1.5	0.0	-1.5	-3.0	-4.5

0.0160	**0.0125**	**0.0100**
-5.9	-7.5	-9.0

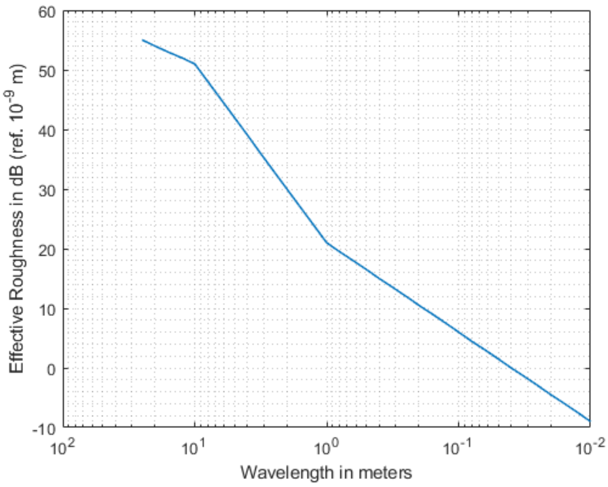

Figure A.3: The HS2 effective roughness function of Table A.3 plotted over wave-length.

Table A.4: Propagation coefficients J & K for surface trains over the HS2 defined generic lithologies (Table 7, Annex D1 in [6]).

	1/3rd Oct. Band (Hz)	**6.3**	**8**	**10**	**12**	**15**	**20**	**25**	**31.5**	**40**	**50**	**63**	**80**	**100**	**125**	**160**	**200**	**250**
Lith-ology:	**Coeff.:**	-	-	-	-	-	-	-	-	-								
Chalk	J	2.50	-2.50	-0.60	3.00	2.50	-8.10	-7.30	-9.60	-21.40	-29.4	-26.6	-28.5	-32.1	-38.9	-40.3	-	-
Chalk	K	-0.14	-0.09	-0.11	-0.15	-0.16	-0.1	-0.19	-0.22	-0.06	0.00	-0.02	0.00	0.00	0.00	0.00	0.00	0.00
Sand	J	-4.20	-9.30	-16.00	-11.00	-9.90	-8.70	-24.10	-26.40	-32.10	-29.40	-34.20	-26.80	-22.30	-17.90	0.00	0.00	0.00
Sand	K	-0.02	0.02	0.03	-0.02	-0.06	-0.17	-0.02	0.00	0.00	-0.05	0.00	0.00	0.00	0.00	0.00	0.00	0.00
Sand & clay	J	-6.60	6.00	8.00	6.40	15.30	-14.10	-8.00	-48.80	-37.80	-38.10	-42.80	-34.80	-31.60	-25.00	-29.60	0.00	0.00
Sand & clay	K	-0.14	-0.21	-0.25	-0.28	-0.42	-0.22	-0.26	0.00	-0.09	-0.06	0.00	0.00	0.00	0.00	0.00	0.00	0.00
Clay	J	-9.53	-9.53	-9.53	-9.53	-9.53	-9.53	-28.60	-38.00	-37.50	-25.40	-42.80	-34.80	-31.60	-25.00	-29.60	0.00	0.00
Clay	K	-0.04	-0.04	-0.04	-0.04	-0.04	-0.04	0.00	0.00	0.00	0.00	0.00	0.00	0.00	0.00	0.00	0.00	0.00

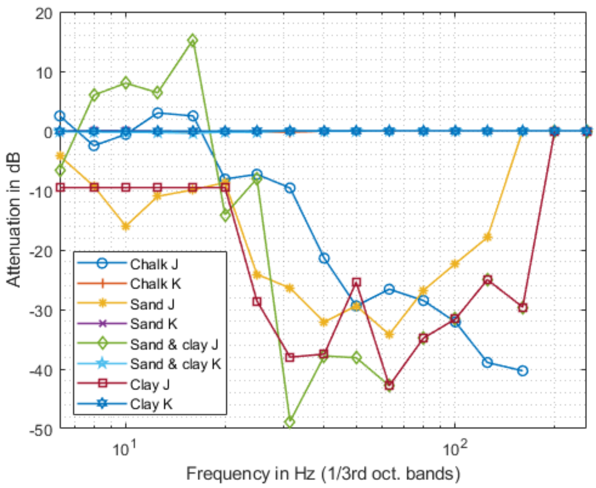

Figure A.4: The HS2 propagation coefficients J & K for surface trains, Table A.4. Attenuation in dB within one third octave bands.

DEPARTMENT OF ARCHITECTURE AND CIVIL ENGINEERING
CHALMERS UNIVERSITY OF TECHNOLOGY
Gothenburg, Sweden
www.chalmers.se

CHALMERS
UNIVERSITY OF TECHNOLOGY